Title	Improved quantum algorithm for calculating eigenvalues of differential operators and its application to estimating the decay rate of the perturbation distribution tail in stochastic inflation
Author(s)	Miyamoto, Koichi; Tada, Yuichiro
Citation	Physical Review Research. 2025, 7, p. 023251
Version Type	VoR
URL	https://hdl.handle.net/11094/102912
rights	This article is licensed under a Creative Commons Attribution 4.0 International License.
Note	

Improved quantum algorithm for calculating eigenvalues of differential operators and its application to estimating the decay rate of the perturbation distribution tail in stochastic inflation

Koichi Miyamoto [1,*] and Yuichiro Tada [2,3,†]

[1] *Center for Quantum Information and Quantum Biology, Osaka University, Toyonaka 560-0043, Japan*
[2] *Institute for Advanced Research, Nagoya University, Furo-cho, Chikusa-ku, Nagoya 464-8601, Japan*
[3] *Department of Physics, Nagoya University, Furo-cho, Chikusa-ku, Nagoya 464-8602, Japan*

Quantum algorithms for scientific computing and their applications have been actively studied. In this paper, we propose a quantum algorithm for estimating the first eigenvalue of a differential operator $\mathcal{L}$ on $\mathbb{R}^d$ and its application to cosmic inflation theory. A common approach for this eigenvalue problem involves applying the finite-difference discretization to $\mathcal{L}$ and computing the eigenvalues of the resulting matrix, but this method suffers from the curse of dimensionality, namely, the exponential complexity with respect to d. Our first contribution is the development of a quantum algorithm for this task, leveraging recent quantum singular value transformation-based methods. Given a trial function that overlaps well with the eigenfunction, our method runs with query complexity scaling as $\widetilde{O}(d^3/\epsilon^2)$ with d and estimation accuracy ϵ, which is polynomial in d and shows improvement over existing quantum algorithms. Then, we consider the application of our method to a problem in a theoretical framework for cosmic inflation known as stochastic inflation, specifically calculating the eigenvalue of the adjoint Fokker–Planck operator, which is related to the decay rate of the tail of the probability distribution for the primordial density perturbation. We numerically see that, in some cases, simple trial functions overlap well with the first eigenfunction, indicating our method is promising for this problem.

I. INTRODUCTION

Today, we are witnessing the rapid development of quantum computing. Although it may take decades for us to obtain large-scale fault-tolerant quantum computers, to prepare for such a future, the search for applications of quantum algorithms to practical numerical problems across various fields has increasingly gained momentum in recent years. In this paper, we consider a quantum algorithm for calculating eigenvalues of differential operators and its application to a problem in cosmology.

With the Sturm–Liouville problem as a representative example, the calculation of eigenvalues of linear partial differential operators, especially the first (that is, smallest) eigenvalue, is one of the major topics in the field of numerical analysis for partial differential equations (PDEs) (see Ref. [1] as a textbook). As is the case for many problems in numerical analysis, this problem suffers from the so-called curse of dimensionality. To calculate the eigenvalues of a linear partial differential operator $\mathcal{L}$ acting on functions on $\mathbb{R}^d$, a straightforward approach is the finite difference approximation: setting grid points in $\mathbb{R}^d$, we approximate partial derivatives with difference quotients. This converts $\mathcal{L}$ to a matrix L with finite size, and then we can apply some numerical method for matrix eigenvalue calculation to L (see, e.g., Ref. [2]). However, the size of L becomes exponentially large with respect to the dimension d, that is, $n_{\mathrm{gr}}^d \times n_{\mathrm{gr}}^d$, where n_{gr} is the number of the grids in one dimension. Since classical algorithms to calculate eigenvalues of a $n \times n$ matrix generally have the complexity scaling as $O(\mathrm{poly}(n))$, the above approach does not work for large d in classical computing.

Quantum computers may provide a solution to this issue. Represented by the monumental Harrow–Hassidim–Lloyd algorithm for solving linear equation systems [3], quantum algorithms for various linear algebra problems have been devised. Algorithms for eigenvalue calculation are among them [4–11]. They achieve an exponential speedup compared to the classical ones: their complexities scale as $O(\mathrm{polylog}(n))$. Therefore, we are motivated to apply these quantum algorithms to the aforementioned finite difference approach for differential operator eigenvalue problems. In fact, such quantum methods have already been considered in previous papers [12–14]. However, to the best of our knowledge, quantum algorithms for differential operator eigenvalue problems have been studied only in the above papers in the 2000s, and among them, only Ref. [12] considered the multidimensional setting and evaluated the complexity of their algorithm in it. Thus, recent developments in quantum algorithms have not been reflected in this problem yet.

In this paper, we first construct a quantum algorithm for calculating differential operator eigenvalues in a modern way. Concretely, we utilize the quantum algorithm for calculating matrix eigenvalues devised in Ref. [9]. This algorithm is

---

*Contact author: miyamoto.kouichi.qiqb@osaka-u.ac.jp
†Contact author: tada.yuichiro.y8@f.mail.nagoya-u.ac.jp

based on the recent techniques of block-encoding and quantum singular value transformation (QSVT) [6,7,10,15,16], which have been foundations of various quantum algorithms. We then combine this algorithm with the finite difference approach for differential operator eigenvalues. Given a test function that overlaps the first eigenfunction well, a quantum circuit to generate the quantum state encoding that functions and circuits to calculate the coefficients in $\mathcal{L}$, our algorithm outputs an estimate of the first eigenvalue, where the above circuits are queried a number of times, scaling polynomially with respect to d and as $\widetilde{O}(1/\epsilon^2)$[1] with respect to the estimation accuracy ϵ. Our quantum algorithm achieves an exponential speedup with respect to d compared to classical algorithms and improvement with respect to ϵ compared to the method in Ref. [12], whose query complexity is $\widetilde{O}(1/\epsilon^3)$.

As the second contribution, we consider a problem in cosmology: the estimation of the decay rate of the tail of the probability distribution of the perturbation in stochastic inflation. Cosmic inflation [17–22], the accelerated expansion of the early universe, was introduced as a solution to some problems in the big bang cosmology and is a standard paradigm today. It is considered that the quantum fluctuation of inflatons, the scalar fields that induced inflation, leads to the primordial density perturbation, which is the seed of today's rich structures of the universe such as galaxies. Stochastic inflation [23–32] is the formalism to analyze the inflationary perturbation in a probabilistic way. In stochastic inflation, the fluctuations of the inflatons are associated with a PDE called the adjoint Fokker-Planck (FP) PDE, and the eigenvalues of the differential operator in it determine the decay rate of the tail of the perturbation distribution. In particular, as an interesting scenario, if there are small eigenvalues, the tail becomes fat, and primordial black holes, a candidate for dark matter, are produced abundantly, which motivates us to estimate the first eigenvalue. Our quantum algorithm may thus be useful for this task, especially in multifield inflation, where the number of inflatons is large and the differential operator is high-dimensional.

Since we do not have fault-tolerant quantum computers yet, we cannot run our algorithm for the above problem. Instead, to see that our algorithm is promising, we numerically check that the overlap condition holds. That is, for some cases with a small enough number of inflatons to be classically dealt with in the finite difference approach, we observe that the first eigenfunction has a considerable overlap with a simple test function of Gaussian shape. This result implies that we can prepare the inputs of our algorithm for the stochastic inflation problem and thus run it on future fault-tolerant quantum computers.

This paper is organized as follows. Section II is a preliminary one, where we present the basics of the finite difference method for calculating eigenvalues of differential operators and some quantum algorithms used as building blocks in this paper. In Sec. III, we present our algorithm for estimating differential operator eigenvalues and evaluate its query complexity. Section IV is devoted to the numerical demonstration concerning the application of our algorithm to the eigenvalue

estimation in stochastic inflation. After we present the basics of stochastic inflation, we see the considerable overlap between the eigenfunctions and the test functions in some cases. This paper ends with the summary in Sec. V.

II. PRELIMINARY

A. Notation

$\mathbb{R}_+$ denotes the set of all non-negative real numbers: $\mathbb{R}_+ := \{x \in \mathbb{R} \mid x > 0\}$.

For $n \in \mathbb{N}$, we define $[n] := \{1, \ldots, n\}$ and $[n]_0 := \{0, 1, \ldots, n-1\}$.

We label entries in a vector and rows and columns in a matrix with integers starting from 0. That is, we write $\mathbf{v} \in \mathbb{C}^n$ as $\mathbf{v} = (v_0, \ldots, v_{n-1})^T$ and $A \in \mathbb{C}^{m \times n}$ as $A = \begin{pmatrix} a_{0,0} & \cdots & a_{0,n-1} \\ \vdots & \ddots & \vdots \\ a_{m-1,0} & \cdots & a_{m-1,n-1} \end{pmatrix}$ entrywise.

For $n \in \mathbb{N}$, I_n denotes the $n \times n$ identity matrix. We may omit the subscript n if there is no ambiguity.

For $\mathbf{v} \in \mathbb{C}^n$, $\|\mathbf{v}\|$ denotes its Euclidean norm. For an (unnormalized) quantum state $|\psi\rangle$ on a multiqubit system, $\|\,|\psi\rangle\,\|$ denotes the Euclidean norm of its state vector. For $A \in \mathbb{C}^{m \times n}$, $\|A\|$ denotes its spectral norm. $\|\mathbf{v}\|_{\max}$ (respectively, $\|A\|_{\max}$) denotes the max norm of $\mathbf{v}$ (respectively, A), which means the maximum of the absolute values of its entries.

For $\epsilon > 0$, we say that $x' \in \mathbb{R}$ is an ϵ approximation of $x \in \mathbb{R}$, if $|x' - x| \leqslant \epsilon$ holds. We also say that x' is ϵ close to x.

If $A \in \mathbb{C}^{m \times n}$ has at most s nonzero entries in each row and column, we say that A is s sparse and the sparsity of A is s.

For a function $f : \Omega \to \mathbb{R}$ on $\Omega \in \mathbb{R}^d$ and $\boldsymbol{\alpha} = (\alpha_1, \ldots, \alpha_d) \in \mathbb{N}^d$, we define

$$|\boldsymbol{\alpha}| := \alpha_1 + \cdots \alpha_d \tag{1}$$

and

$$D^{\boldsymbol{\alpha}} f := \frac{\partial^{|\boldsymbol{\alpha}|} f}{\partial x_1^{\alpha_1} \cdots \partial x_d^{\alpha_d}}. \tag{2}$$

We denote by 1_C the indicator function, which takes 1 if the condition C is satisfied and 0 otherwise.

B. Approximating eigenvalues of a differential operator by the finite difference method

We now formulate the eigenvalue problem for a differential operator, focusing on the Sturm–Liouville type, to which the eigenvalue problem in stochastic inflation also boils down.

Problem 1. Consider

$$\mathcal{L} = -\sum_{i=1}^{d} \frac{\partial}{\partial x_i}\left(a_i \frac{\partial}{\partial x_i} \right) + a_0 \tag{3}$$

a linear second-order self-adjoint elliptic differential operator on $\mathcal{D} := (L, U) \times \cdots \times (L, U) \subset \mathbb{R}^d$, where $a_0, a_1, \ldots, a_d : \overline{\mathcal{D}} \to \mathbb{R}_+$ are four times continuously differentiable on $\overline{\mathcal{D}}$. We consider the eigenvalue problem for $\mathcal{L}$ with the Dirichlet boundary condition: We aim to find real numbers $\lambda_1 \leqslant \lambda_2 \leqslant \cdots$, each of which satisfies

$$\mathcal{L} f_k(\mathbf{x}) = \lambda_k f_k(\mathbf{x}); \quad \text{for } \mathbf{x} \in \mathcal{D}$$
$$f_k(\mathbf{x}) = 0; \quad \text{for } \mathbf{x} \in \partial \mathcal{D} \tag{4}$$

---

[1] $\widetilde{O}(\cdot)$ hides the logarithmic factors in Landau's big-O notation.

for some function $f_k : \overline{\mathcal{D}} \to \mathbb{R}$, especially the smallest one λ_1.

We call each λ_k an eigenvalue of $\mathcal{L}$ and f_k the eigenfunction of $\mathcal{L}$ corresponding to λ_k. We denote by $\mathcal{F}_{\mathcal{L}}$ the space of functions spanned by eigenfunctions of $\mathcal{L}$.

For this problem, we take a finite difference-based approach. We start by setting grid points in $\overline{\mathcal{D}}$. We take an integer $n_{\mathrm{gr}} \in \mathbb{N}$, which means the number of grid points in each of the d dimensions, and denote by $N_{\mathrm{gr}} := n_{\mathrm{gr}}^d$ the total number of grid points in $\mathcal{D}$. We set the grid point interval $h := (U - L)/(n_{\mathrm{gr}} + 1)$. We take the grid point set $\mathcal{D}_{n_{\mathrm{gr}}}$, which consists of the points $\mathbf{x}_{\mathbf{j}}^{\mathrm{gr}} \in \mathcal{D}$ labeled by $\mathbf{j} = (j_1, \ldots, j_d)^T \in [n_{\mathrm{gr}}]_0^d$ and written as

$$
\begin{aligned}
\mathbf{x}_{\mathbf{j}}^{\mathrm{gr}} &= \left(x_{1,j_1}^{\mathrm{gr}}, \ldots, x_{d,j_d}^{\mathrm{gr}}\right)^T, \\
x_{i,j_i}^{\mathrm{gr}} &= (j_i + 1)h + L \quad \text{for each } i \in [d].
\end{aligned}
\tag{5}
$$

We label the point $\mathbf{x}_{\mathbf{j}}^{\mathrm{gr}}$ also by an integer $J = J(\mathbf{j})$, where

$$
J(\mathbf{j}) := \sum_{i=1}^d n_{\mathrm{gr}}^{i-1} j_i,
\tag{6}
$$

and denote it also by $\mathbf{x}_J^{\mathrm{gr}}$. Hereafter, we sometimes label entries in a vector $v \in \mathbb{C}^{N_{\mathrm{gr}}}$ and rows and columns in a matrix $A \in \mathbb{C}^{N_{\mathrm{gr}} \times N_{\mathrm{gr}}}$ with $\mathbf{j} \in [n_{\mathrm{gr}}]_0^d$, where the one labeled by $\mathbf{j}$ corresponds to the $J(\mathbf{j})$th one: e.g., $v_{\mathbf{j}}$ is the $J(\mathbf{j})$th entry in the vector $(v_0, \ldots, v_{N_{\mathrm{gr}}-1})^T$.

Using these grid points, we construct a finite difference approximation $L_{n_{\mathrm{gr}}}$ of $\mathcal{L}$. That is, we want a $N_{\mathrm{gr}} \times N_{\mathrm{gr}}$ real symmetric matrix $L_{n_{\mathrm{gr}}}$ that satisfies

$$
\left| \left(L_{n_{\mathrm{gr}}} \mathbf{v}_{f,n_{\mathrm{gr}}}\right)_{\mathbf{j}} - \mathcal{L}f\left(\mathbf{x}_{\mathbf{j}}^{\mathrm{gr}}\right) \right| \xrightarrow{n_{\mathrm{gr}} \to \infty} 0
\tag{7}
$$

for any $f \in \mathcal{F}_{\mathcal{L}}$ and any $\mathbf{j} \in [n_{\mathrm{gr}}]_0^d$. Here, for $f : \overline{\mathcal{D}} \to \mathbb{R}$, we define $\mathbf{v}_{f,n_{\mathrm{gr}}} \in \mathbb{R}^{N_{\mathrm{gr}}}$ as

$$
\mathbf{v}_{f,n_{\mathrm{gr}}} := \left(f\left(\mathbf{x}_0^{\mathrm{gr}}\right), \ldots, f\left(\mathbf{x}_{N_{\mathrm{gr}}-1}^{\mathrm{gr}}\right)\right)^T.
\tag{8}
$$

Specifically, we take $L_{n_{\mathrm{gr}}}$ as follows: For $\mathbf{j}_1, \mathbf{j}_2 \in [n_{\mathrm{gr}}]_0^d$, its $(\mathbf{j}_1, \mathbf{j}_2)$th entry is

$$
\left(L_{n_{\mathrm{gr}}}\right)_{\mathbf{j}_1, \mathbf{j}_2} = \begin{cases} \sum_{i=1}^d \frac{a_i\left(\mathbf{x}_{\mathbf{j}_1}^{\mathrm{gr}} + \frac{h}{2}\mathbf{e}_i\right) + a_i\left(\mathbf{x}_{\mathbf{j}_1}^{\mathrm{gr}} - \frac{h}{2}\mathbf{e}_i\right)}{h^2} + a_0\left(\mathbf{x}_{\mathbf{j}_1}^{\mathrm{gr}}\right), & \text{if } \mathbf{j}_1 = \mathbf{j}_2, \\ -\frac{a_i\left(\mathbf{x}_{\mathbf{j}_1}^{\mathrm{gr}} \pm \frac{h}{2}\mathbf{e}_i\right)}{h^2}, & \text{if } \mathbf{j}_2 = \mathbf{j}_1 \pm \mathbf{e}_i \text{ for some } i \in [d], \\ 0, & \text{otherwise,} \end{cases}
\tag{9}
$$

where $\mathbf{e}_i \in \mathbb{R}^d$ is a vector with all entries equal to 0 except for the ith entry equal to 1. In other words, for $\mathbf{j} \in [n_{\mathrm{gr}}]_0^d$,

$$
\begin{aligned}
\left(L_{n_{\mathrm{gr}}} \mathbf{v}_{f,n_{\mathrm{gr}}}\right)_{\mathbf{j}} = \sum_{i=1}^d \frac{1}{h^2} \Bigg[&-a_i\left(\mathbf{x}_{\mathbf{j}}^{\mathrm{gr}} + \frac{h}{2}\mathbf{e}_i\right) f\left(\mathbf{x}_{\mathbf{j}}^{\mathrm{gr}} + h\mathbf{e}_i\right) + \left(a_i\left(\mathbf{x}_{\mathbf{j}}^{\mathrm{gr}} + \frac{h}{2}\mathbf{e}_i\right) + a_i\left(\mathbf{x}_{\mathbf{j}}^{\mathrm{gr}} - \frac{h}{2}\mathbf{e}_i\right)\right) f\left(\mathbf{x}_{\mathbf{j}}^{\mathrm{gr}}\right) \\
&-a_i\left(\mathbf{x}_{\mathbf{j}}^{\mathrm{gr}} - \frac{h}{2}\mathbf{e}_i\right) f\left(\mathbf{x}_{\mathbf{j}}^{\mathrm{gr}} - h\mathbf{e}_i\right) \Bigg] + a_0(\mathbf{x}) f\left(\mathbf{x}_{\mathbf{j}}^{\mathrm{gr}}\right).
\end{aligned}
\tag{10}
$$

This $L_{n_{\mathrm{gr}}}$ is based on the following formula (see Sec. 6.2 in Ref. [1]):

$$
\frac{\partial}{\partial x_i}\left(a_i \frac{\partial f}{\partial x_i}\right)(\mathbf{x}) = \frac{1}{h^2}\left[a_i\left(\mathbf{x} + \frac{h}{2}\mathbf{e}_i\right) f(\mathbf{x} + h\mathbf{e}_i) - \left(a_i\left(\mathbf{x} + \frac{h}{2}\mathbf{e}_i\right) + a_i\left(\mathbf{x} - \frac{h}{2}\mathbf{e}_i\right)\right) f(\mathbf{x}) + a_i\left(\mathbf{x} - \frac{h}{2}\mathbf{e}_i\right) f(\mathbf{x} - h\mathbf{e}_i)\right] + O(h^2),
\tag{11}
$$

which holds for any sufficiently smooth function f.

Then, we expect that the eigenvalues of $L_{n_{\mathrm{gr}}}$ approximate those of $\mathcal{L}$ for sufficiently large n_{gr} and, in fact, this holds. We have the following theorem by applying Theorem 5.1 in Ref. [33] to the current case.

Theorem 1. For each $k \in \mathbb{N}$, there exist constants $C_{\mathcal{L}}^k, D_{\mathcal{L}}^k \in \mathbb{R}$ determined only by k and $\mathcal{L}$ such that, for any $n_{\mathrm{gr}} \in \mathbb{N}$, and the following hold:

(1)

$$
\left|\lambda_{n_{\mathrm{gr}}}^k - \lambda_k\right| \leqslant \frac{C_{\mathcal{L}}^k}{n_{\mathrm{gr}}^2},
\tag{12}
$$

where $\lambda_{n_{\mathrm{gr}}}^1 \leqslant \lambda_{n_{\mathrm{gr}}}^2 \leqslant \cdots$ are the eigenvalues of $L_{n_{\mathrm{gr}}}$.

(2) For any eigenvector $\mathbf{v}_{n_{\mathrm{gr}}}^k$ of $L_{n_{\mathrm{gr}}}$ that corresponds to $\lambda_{n_{\mathrm{gr}}}^k$ and is normalized as $\|\mathbf{v}_{n_{\mathrm{gr}}}^k\|_{n_{\mathrm{gr}}} = 1$, there exists an eigenfunc-

tion f_k of $\mathcal{L}$ corresponding to λ_k that satisfies

$$
\left\|\mathbf{v}_{n_{\mathrm{gr}}}^k - \mathbf{v}_{f_k,n_{\mathrm{gr}}}\right\|_{\max} \leqslant \frac{D_{\mathcal{L}}^k}{n_{\mathrm{gr}}^2}.
\tag{13}
$$

Here, for $\mathbf{v} = (v_0, \ldots, v_{N_{\mathrm{gr}}-1}) \in \mathbb{C}^{N_{\mathrm{gr}}}$, $\|\mathbf{v}\|_{n_{\mathrm{gr}}} := h^d \sum_{J=0}^{N_{\mathrm{gr}}-1} |v_J|^2$.

The proof is given in Appendix 1.

C. Building-block quantum algorithms

1. Arithmetic circuits

In this paper, we consider computation on the system with multiple quantum registers. We use the fixed-point binary representation for real numbers and, for each $x \in \mathbb{R}$, we denote by $|x\rangle$ the computational basis state on a quantum register where the bit string corresponds to the binary representation of x. We

assume that every register has a sufficient number of qubits and thus neglect errors by finite precision representation.

We can perform arithmetic operations on numbers represented on qubits. For example, we can implement quantum circuits for four basic arithmetic operations: addition $O_{\mathrm{add}} : |a\rangle |b\rangle |0\rangle \mapsto |a\rangle |b\rangle |a+b\rangle$, subtraction $O_{\mathrm{sub}} : |a\rangle |b\rangle |0\rangle \mapsto |a\rangle |b\rangle |a-b\rangle$, multiplication $O_{\mathrm{mul}} : |a\rangle |b\rangle |0\rangle \mapsto |a\rangle |b\rangle |ab\rangle$, and division $O_{\mathrm{div}} : |a\rangle |b\rangle |0\rangle |0\rangle \mapsto |a\rangle |b\rangle |q\rangle |r\rangle$, where $a, b \in \mathbb{Z}$ and q and r are the quotient and remainder of a/b, respectively. For concrete implementations, see Ref. [34] and the references therein. In the finite precision binary representation, these operations are immediately extended to those for real numbers. Moreover, using the above circuits, we can also construct a circuit to compute an elementary function f such as an exponential as $O_f : |x\rangle |0\rangle \mapsto |x\rangle |f(x)\rangle$; see Ref. [35] for the details of the construction. Hereafter, we collectively call these circuits arithmetic circuits. The gate cost of such a circuit is polynomial with respect to the number of digits in binary representation and not related to the parameters in the currently considered problem such as ϵ, as long as a sufficient number of digits are used. Thus, we regard their contributions as constant in the complexity evaluation conducted later. That is, in such an evaluation, we regard them as a unit and count the number of queries to them and circuits constructed by their combinations [e.g., O_{a_i} in Eq. (27)].

2. Representation of a vector as a quantum state

For a vector $\mathbf{v} = (v_0, \ldots, v_{n-1}) \in \mathbb{R}^n$, we consider the two ways to encode it into a quantum state. The first one is amplitude encoding: We define

$$|\mathbf{v}\rangle := \frac{1}{\sqrt{\sum_{i=0}^{n-1} v_i^2}} \sum_{i=0}^{n-1} v_i |i\rangle. \tag{14}$$

We will later consider quantum states like this for vectors like $\mathbf{v}_{f, n_{\mathrm{gr}}}$, which consists of the values of functions at grid points. For a function written by some explicit formula, there are various methods to generate an amplitude-encoding state [36–43].

The second way is binary encoding: We define

$$|\mathbf{v}\rangle_{\mathrm{bin}} := |v_0\rangle \cdots |v_{n-1}\rangle. \tag{15}$$

3. Block encoding

Block encoding means embedding a general matrix into the upper-left block of a unitary matrix.

Definition 1 (Ref. [7], Definition 24). Let $n, a \in \mathbb{N}$, $A \in \mathbb{C}^{2^n \times 2^n}$, $\epsilon \in \mathbb{R}_+$, and $\alpha \geqslant \|A\|$. We say that a unitary U on a $(n+a)$-qubit system is an (α, a, ϵ)-block encoding of A, if

$$\|A - \alpha(\langle 0|^{\otimes a} \otimes I_{2^n}) U (|0\rangle^{\otimes a} \otimes I_{2^n})\| \leqslant \epsilon. \tag{16}$$

We can efficiently construct a block encoding of a matrix A if we have sparse access to A, that is, if A is sparse and we can query quantum circuits that output positions and values of nonzero entries in A.

Theorem 2 (Ref. [7], Lemma 48 in the full version, modified). Let $A = (A_{ij}) \in \mathbb{C}^{2^n \times 2^n}$ be an s-sparse matrix. Suppose that we have access to oracles O_{row}^A and O_{col}^A that act on a

two-register system as

$$O_{\mathrm{row}}^A |i\rangle |k\rangle = |i\rangle |r_{ik}\rangle, \quad O_{\mathrm{col}}^A |k\rangle |i\rangle = |c_{ki}\rangle |i\rangle \tag{17}$$

for any $i \in [2^n]_0$ and $k \in [s]$, where r_{ik} (respectively, c_{ki}) is the index of the kth nonzero entry in the ith row (respectively, column) in A, or $i + 2^n$ if there are less than k nonzero entries. In addition, suppose that we have access to oracle O_{ent}^A that acts on a three-register system as

$$O_{\mathrm{ent}}^A |i\rangle |j\rangle |0\rangle = |i\rangle |j\rangle |A_{ij}\rangle. \tag{18}$$

Then, for any $\epsilon \in \mathbb{R}_+$, there exists a $(s\|A\|_{\max}, n+3, \epsilon)$-block encoding of A, in which O_{row}^A and O_{col}^A are each queried once, O_{ent}^A is queried twice, additional $O(n + \log^{5/2}(\frac{s^2\|A\|_{\max}}{\epsilon}))$ one- and two-qubit gates are used, and $O(\log^{5/2}(\frac{s^2\|A\|_{\max}}{\epsilon}))$ ancilla qubits are used.

4. Estimation of the smallest eigenvalue of a Hermitian

Given a block encoding of matrix A, we can use QSVT [7,10] to construct a block encoding of another matrix $\tilde{A}$ obtained via transforming the singular values of A by a polynomial f satisfying some conditions. For a Hermitian H, this corresponds to transforming its eigenvalues, and various operations concerning the eigenvalues are possible via QSVT. Reference [9] utilized this scheme to construct a quantum algorithm to estimate the smallest eigenvalue of a hermitian.

Theorem 3 (Ref. [9], Theorem 8). Let H be a $2^n \times 2^n$ Hermitian with the smallest eigenvalue λ_1 and the corresponding eigenvector $|\psi_1\rangle$. Suppose that we have access to $(\alpha, a, 0)$-block encoding U_H of H. Also suppose that we have access to the unitary $U_{|\phi_1\rangle}$ on an n-qubit system to generate a state $|\phi_1\rangle$, that is, $U_{|\phi_1\rangle} |0\rangle = |\phi_1\rangle$, where $|\langle \phi_1 | \psi_1 \rangle| \geqslant \gamma$ holds with some $\gamma > 0$. Then, for any $\delta \in (0, 1)$ and $\epsilon > 0$, there exists a quantum algorithm that outputs an ϵ approximation of λ_1 with probability at least $1 - \delta$, using

$$O\left(\frac{\alpha}{\gamma\epsilon} \log\left(\frac{\alpha}{\epsilon}\right) \log\left(\frac{1}{\gamma}\right) \log\left(\frac{\log(\alpha/\epsilon)}{\delta}\right)\right) \tag{19}$$

times, $U_{|\phi_0\rangle}$

$$O\left(\frac{1}{\gamma} \log\left(\frac{\alpha}{\epsilon}\right) \log\left(\frac{\log(\alpha/\epsilon)}{\delta}\right)\right) \tag{20}$$

times,

$$O\left(\frac{a\alpha}{\gamma\epsilon} \log\left(\frac{\alpha}{\epsilon}\right) \log\left(\frac{1}{\gamma}\right) \log\left(\frac{\log(\alpha/\epsilon)}{\delta}\right)\right) \tag{21}$$

additional one- and two-qubit gates, and

$$O\left(n + a + \log\left(\frac{1}{\gamma}\right)\right) \tag{22}$$

qubits.

We can modify the quantum algorithm in Ref. [9], for which the availability of an exact block encoding of H is assumed, to an algorithm built upon sparse access to H and thus an approximate block encoding of it.

Corollary 1. Let the assumptions in Theorem 3 hold, except that on the $(\alpha, a, 0)$-block encoding of H replaced with the following: H is s sparse; we have access to O_{row}^H, O_{col}^H, and O_{ent}^H that act as Eqs. (17) and (18) with $A = H$. Then, for

any $\delta \in (0, 1)$ and $\epsilon > 0$, there exists a quantum algorithm $\mathsf{EstEig}(H, \epsilon, \delta)$ that outputs an ϵ approximation of λ_1 with probability at least $1 - \delta$, using O_{row}^H, O_{col}^H, and O_{ent}^H,

$$O\left(\frac{s \|H\|_{\max}}{\gamma \epsilon} \log \left(\frac{s \|H\|_{\max}}{\epsilon} \right) \log \left(\frac{1}{\gamma} \right) \right.$$
$$\left. \times \log \left(\frac{\log(s \|H\|_{\max}/\epsilon)}{\delta} \right) \right) \qquad (23)$$

times, $U_{|\phi_0\rangle}$,

$$O\left(\frac{1}{\gamma} \log \left(\frac{s \|H\|_{\max}}{\epsilon} \right) \log \left(\frac{\log(s \|H\|_{\max}/\epsilon)}{\delta} \right) \right) \qquad (24)$$

times,

$$O\left(\frac{s \|H\|_{\max}}{\gamma \epsilon} \log \left(\frac{s \|H\|_{\max}}{\epsilon} \right) \log \left(\frac{1}{\gamma} \right) \right.$$
$$\times \log \left(\frac{\log(s \|H\|_{\max}/\epsilon)}{\delta} \right)$$
$$\left. \times \left(n + \log^{5/2} \left(\frac{s^3 \|H\|_{\max}^2 \log^2(1/\gamma)}{\gamma^2 \epsilon^2} \right) \right) \right) \qquad (25)$$

additional one- and two-qubit gates, and

$$O\left(n + \log \left(\frac{1}{\gamma} \right) + \log^{5/2} \left(\frac{s^3 \|H\|_{\max}^2 \log^2(1/\gamma)}{\gamma^2 \epsilon^2} \right) \right) \qquad (26)$$

qubits.

Proof. See Appendix 2. ∎

III. IMPROVED QUANTUM ALGORITHM FOR EIGENVALUE ESTIMATION FOR DIFFERENTIAL OPERATORS

Now, let us present our quantum algorithm for estimating the smallest eigenvalue of a differential operator $\mathcal{L}$ in the form of Eq. (3). We begin by making assumptions about access to quantum circuits used in our algorithms. The first one is the circuits to compute the coefficient a_i in $\mathcal{L}$.

Assumption 1. For each $i \in \{0, 1, \ldots, d\}$, we have access to a quantum circuit O_{a_i} that acts as

$$O_{a_i} |\mathbf{x}\rangle_{\text{bin}} |0\rangle = |\mathbf{x}\rangle_{\text{bin}} |a_i(\mathbf{x})\rangle \qquad (27)$$

for any $\mathbf{x} \in \mathcal{D}$.

As long as a_i is given by some explicit formula, which is the case in the stochastic inflation case considered below, O_{a_i} can be implemented with arithmetic circuits.

The second one is the circuit to generate the quantum state that encodes the test function, which is chosen in advance and assumed to overlap well with the first eigenfunction of $\mathcal{L}$.

Assumption 2. Let $\gamma \in (0, 1)$. For any $n_{\text{gr}} \in \mathbb{N}$, we have access to a quantum circuit $O_{\tilde{f}_1, n_{\text{gr}}}$ that acts as

$$O_{\tilde{f}_1, n_{\text{gr}}} |0\rangle = |\mathbf{v}_{\tilde{f}_1, n_{\text{gr}}}\rangle, \qquad (28)$$

where $\tilde{f}_1 : \mathcal{D} \to \mathbb{R}$ is a function on $\mathcal{D}$ and satisfies

$$\left| \langle \mathbf{v}_{\tilde{f}_1, n_{\text{gr}}} | \mathbf{v}_{f_1, n_{\text{gr}}} \rangle \right| \geqslant \gamma. \qquad (29)$$

As mentioned in Sec. II C 2, for the function $\tilde{f}_1$ written by an explicit formula, there are various proposals on the way to

generate the state $|\mathbf{v}_{\tilde{f}_1, n_{\text{gr}}}\rangle$, and we now assume that some of them are available.

Then, we present the main theorem on our quantum algorithm.

Theorem 4. Consider Problem 1 under Assumptions 1 and 2. Let $\epsilon \in \mathbb{R}$ and $\delta \in (0, 1)$. Then, there exists a quantum algorithm that outputs an ϵ-approximation of λ_1 with probability at least $1 - \delta$, making

$$O\left(\frac{d\xi}{\gamma} \log \xi \log \left(\frac{1}{\gamma} \right) \log \left(\frac{\log \xi}{\delta} \right) \right) \qquad (30)$$

uses of $O_{a_0}, \ldots, O_{a_d}$ and arithmetic circuits and

$$O\left(\frac{1}{\gamma} \log \xi \log \left(\frac{\log \xi}{\delta} \right) \right) \qquad (31)$$

uses of $O_{\tilde{f}_1, n_{\text{gr}}}$ with

$$n_{\text{gr}} = \left\lceil \max \left\{ \sqrt{\frac{2C_{\mathcal{L}}^1}{\epsilon}}, \sqrt{\frac{2D_{\mathcal{L}}^1}{1 - \eta(\gamma)}} (U - L)^{d/4} \right\} \right\rceil. \qquad (32)$$

Here,

$$\xi :=$$
$$\frac{d}{\epsilon} \left(\frac{d a_{\max}}{(U - L)^2} \times \max \left\{ \frac{C_{\mathcal{L}}^1}{\epsilon}, \frac{D_{\mathcal{L}}^1 (U - L)^{\frac{d}{2}}}{1 - \eta(\gamma)} \right\} + a_{0,\max} \right), \qquad (33)$$

$$a_{\max} := \max_{\substack{i \in [d] \\ \mathbf{x} \in \overline{\mathcal{D}}}} a_i(\mathbf{x}), \quad a_{0,\max} := \max_{\mathbf{x} \in \overline{\mathcal{D}}} a_0(\mathbf{x}) \qquad (34)$$

and, for $x \in (0, 1)$,

$$\eta(x) := \tfrac{1}{2} (x^2 + \sqrt{4 - 5x^2 + x^4}). \qquad (35)$$

Proof. Here, we just present the quantum algorithm and postpone the rest of the proof, that is, presenting how to construct $O_{\text{row}}^{L_{n_{\text{gr}}}}$, $O_{\text{col}}^{L_{n_{\text{gr}}}}$, and $O_{\text{ent}}^{L_{n_{\text{gr}}}}$, estimating the accuracy of the output and the query complexity estimation, to Appendix 3.

ALGORITHM 1. Estimation of the first eigenvalue λ_1 of $\mathcal{L}$.

Input: Accuracy $\epsilon \in \mathbb{R}$, success probability $1 - \delta \in (0, 1)$.

   1: Set n_{gr} as Eq. (32).
   2: Construct the oracles $O_{\text{row}}^{L_{n_{\text{gr}}}}$, $O_{\text{col}}^{L_{n_{\text{gr}}}}$, and $O_{\text{ent}}^{L_{n_{\text{gr}}}}$.
   3: Run $\mathsf{EstEig}(L_{n_{\text{gr}}}, \frac{\epsilon}{2}, \delta)$ to get an $\frac{\epsilon}{2}$-approximation $\tilde{\Lambda}$ of the smallest eigenvalue of $L_{n_{\text{gr}}}$.
   4: Output $\tilde{\Lambda}$.

∎

Assuming that we can take a good function $\tilde{f}_1$ with $\gamma = \Theta(1)$, we take only the leading part with respect to $\frac{1}{\epsilon}$ to simplify Eq. (30) as

$$\widetilde{O}\left(\frac{d^3 a_{\max} C_{\mathcal{L}}^1}{(U - L)^2 \epsilon^2} \right). \qquad (36)$$

This evaluation can be decomposed into the following contributions. For $L_{n_{\text{gr}}}$, the sparsity is $s = O(d)$, and the max norm is, as seen in Appendix 3, $\|L_{n_{\text{gr}}}\|_{\max} = O(d a_{\max} C_{\mathcal{L}}^1/(U -$

$L)^2\epsilon)$ for small ϵ. Plugging these into Eq. (23) and noting that $O_{\text{row}}^{L_{\text{ngr}}}$, $O_{\text{col}}^{L_{\text{ngr}}}$, and $O_{\text{ent}}^{L_{\text{ngr}}}$ are implemented by $O(d)$ uses of $O_{a_0}, \ldots, O_{a_d}$ and arithmetic circuits as shown in Appendix A 3, we reach Eq. (36).

Let us comment on the improvement of the complexity in our algorithm compared to the previous algorithm in Ref. [12]. That algorithm also takes a kind of finite difference approximation L' for $\mathcal{L}$, which is different from Eq. (9), but the estimation of the eigenvalue of L' is done by the Abrams-Lloyd algorithm [4]. It is the combination of the Hamiltonian simulation with $H = L'$, which means applying the time evolution operator $\exp(-iL't)$ to quantum states and the quantum Fourier transform. Ref. [12] did not present any complexity upper bound of their algorithm that shows the scaling on all the parameters collectively but only stated the scaling of the complexity on the accuracy ϵ. According to it, their algorithm applied to the current problem has the complexity of order $\tilde{O}(1/\epsilon^3)$. This complexity is affected by that of the Hamiltonian simulation method adopted in Ref. [12], which is a kind of Suzuki-Trotter decomposition and not the state-of-the-art method based on QSVT. Compared to this, our algorithm uses the eigenvalue estimation method in Ref. [9], which does not involve the Hamiltonian simulation but is a binary search algorithm utilizing the QSVT-based eigenvalue thresholding. Thus, our algorithm improves the complexity as in Eq. (36).

IV. APPLICATION TO ESTIMATING THE DECAY RATE OF THE PERTURBATION DISTRIBUTION TAIL IN STOCHASTIC INFLATION

We exemplify an application of the quantum algorithm we showed to *cosmic inflation* as physical interest. Cosmic inflation [17–22] is the hypothetical phase of accelerated expansion in the early universe. Not only can it make our universe statistically homogeneous and isotropic from a global perspective, but inflation can also bring primordial fluctuations in energy density or the spacetime metric from the quantum vacuum fluctuation. Such primordial perturbations can be seeds of the current cosmological structures such as galaxies and clusters, and these observations support the existence of inflation (see, e.g., Ref. [44]).

The fluctuating dynamics of inflation is often described in the *stochastic formalism of inflation*, also known as *stochastic inflation* (see Refs. [23–32] for early works and also Ref. [45] for a recent review). It is understood as an effective theory of fields coarse-grained on a superHubble scale. We suppose that inflation is driven by d canonical real scalar fields $\boldsymbol{\phi} = (\phi_1, \phi_2, \cdots \phi_d)$ called *inflatons*. Then, in stochastic inflation, the inflaton fields at each spatial point behave as almost independent stochastic processes. In the so-called slow-roll limit, the stochastic differential equation which the inflatons follow at each spatial point is exhibited as (see, e.g., Ref. [46])

$$d\boldsymbol{\phi}(N) = -M_{\text{Pl}}^2 \frac{\nabla_{\boldsymbol{\phi}} v(\boldsymbol{\phi}(N))}{v(\boldsymbol{\phi}(N))} dN + \sqrt{2v(\boldsymbol{\phi}(N))} dW(N), \quad (37)$$

where M_{Pl} is the reduced Planck mass, $v = V/(24\pi^2 M_{\text{Pl}}^4) : \mathbb{R}^d \to \mathbb{R}$ is the reduced potential of the inflatons, the e-folding number N is the time variable normalized by the Hubble parameter, and $W(N)$ is the d-dimensional Wiener process

independent over the Hubble distance.[2] We omitted the spatial label **x** as hereafter we only deal with the one-point dynamics in this paper.

Due to their stochastic behavior, inflation continues for different times at each spatial point even if the inflaton fields have the same initial value $\boldsymbol{\phi}_0$. Supposing that inflation happens in a certain subset of the target manifold $\Omega \subset \mathbb{R}^I$ and ends at its boundary $\partial\Omega$, the inflation duration is given by the first passage time denoted $\mathcal{N}(\boldsymbol{\phi}_0)$ from $\boldsymbol{\phi}_0$ to $\partial\Omega$. According to the δN formalism [51–57], the fluctuation in this first passage time is understood as the conserved curvature perturbation ζ (fluctuation in the spatial curvature), which is converted to the energy density contrast in the later universe. Its correlation functions over different spatial points, though we do not explicitly calculate them in this paper, are calculated by the probability density function (PDF) of $\mathcal{N}(\boldsymbol{\phi}_0)$ and its dependence on $\boldsymbol{\phi}_0$ known as the *stochastic-$\delta\mathcal{N}$ technique* [46,58–62]. Hence, the problem of interest reduces to solving the PDF of $\mathcal{N}$ from each field value $\boldsymbol{\phi} \in \Omega$, omitting the subscript 0 here and hereafter for simplicity.

The PDF $P(\boldsymbol{\phi} \mid N)$ of the inflatons $\boldsymbol{\phi}$ at a certain time N follows the FP equation equivalent to the original stochastic differential equation (37) as

$$\partial_N P(\boldsymbol{\phi} \mid N) = \mathcal{L}_{\text{FP}} P(\boldsymbol{\phi} \mid N)$$

$$:= M_{\text{Pl}}^2 \left[\sum_i \partial_{\phi_i} \left(\frac{v_i(\boldsymbol{\phi})}{v(\boldsymbol{\phi})} P(\boldsymbol{\phi} \mid N) \right) \right.$$

$$\left. + \sum_i \partial_{\phi_i}^2 (v(\boldsymbol{\phi}) P(\boldsymbol{\phi} \mid N)) \right], \quad (38)$$

where $v_i = \partial_{\phi_i} v$. On the other hand, the PDF of the first passage time $P_{\text{FPT}}(\mathcal{N} \mid \boldsymbol{\phi})$ is known to follow the adjoint one [46]:

$$\partial_{\mathcal{N}} P_{\text{FPT}}(\mathcal{N} \mid \boldsymbol{\phi}) = \mathcal{L}_{\text{FP}}^{\dagger} P_{\text{FPT}}(\mathcal{N} \mid \boldsymbol{\phi}), \quad (39)$$

with the adjoint FP operator

$$\frac{1}{M_{\text{Pl}}^2} \mathcal{L}_{\text{FP}}^{\dagger} = -\sum_i \frac{v_i}{v} \partial_{\phi_i} + v \sum_i \partial_{\phi_i}^2, \quad (40)$$

associated with the inner product,

$$\langle f(\boldsymbol{\phi}) | g(\boldsymbol{\phi}) \rangle := \int d\boldsymbol{\phi} f(\boldsymbol{\phi}) g(\boldsymbol{\phi}), \quad (41)$$

that is, $\langle f(\boldsymbol{\phi}) | \mathcal{L}_{\text{FP}} g(\boldsymbol{\phi}) \rangle = \langle \mathcal{L}_{\text{FP}}^{\dagger} f(\boldsymbol{\phi}) | g(\boldsymbol{\phi}) \rangle$. The eigenvalues of $\mathcal{L}_{\text{FP}}^{\dagger}$ are negative in the set of functions valid as a PDF of the first passage time [63], and we hereafter consider the eigenvalues of $-\mathcal{L}_{\text{FP}}^{\dagger}$, which are positive. Though $\mathcal{L}_{\text{FP}}^{\dagger}$ is not Hermite (not self-adjoint; $\mathcal{L}_{\text{FP}}^{\dagger} \neq \mathcal{L}_{\text{FP}}$), one can Hermitise it

---

[2]The stochastic term should be understood as the Itô integral [47,48]. However, the Itô integral breaks the covariance under the general coordinate transformation on the inflatons' target manifold if it is not Euclidean $\mathbb{R}^d$ but a more general one $\mathcal{M}$ [49]. In such a case, the inflatons' derivative $d\phi_i$ should be replaced by the *Itô-covariant* one. See Ref. [50] for details.

by defining the following Hermitian operator [63]:

$$\widetilde{\mathcal{L}_{\mathrm{FP}}} := w^{1/2}(\boldsymbol{\phi})\mathcal{L}_{\mathrm{FP}}^{\dagger} w^{-1/2}(\boldsymbol{\phi}), \tag{42}$$

where

$$w(\boldsymbol{\phi}) = \mathrm{e}^{1/v(\boldsymbol{\phi})}/v(\boldsymbol{\phi}). \tag{43}$$

They share the same eigenvalues, while the corresponding eigenfunctions are different by the $w^{-1/2}$ factor:

$$-\widetilde{\mathcal{L}_{\mathrm{FP}}}\Psi_n(\boldsymbol{\phi}) = \Lambda_n \Psi_n(\boldsymbol{\phi}) \;\Leftrightarrow\; -\mathcal{L}_{\mathrm{FP}}^{\dagger}\tilde{\Psi}_n(\boldsymbol{\phi}) = \Lambda_n \tilde{\Psi}_n(\boldsymbol{\phi}), \tag{44}$$

where

$$\tilde{\Psi}_n(\boldsymbol{\phi}) = w^{-1/2}(\boldsymbol{\phi})\Psi_n(\boldsymbol{\phi}). \tag{45}$$

By some calculations, we see that

$$-\frac{\widetilde{\mathcal{L}_{\mathrm{FP}}}}{M_{\mathrm{Pl}}^2} = \sum_i \left[-\partial_{\phi_i}(v\partial_{\phi_i}) - \frac{2v^2(1+v)v_{ii} - (1+4v+v^2)v_i^2}{4v^3} \right], \tag{46}$$

where $v_{ii} := \partial_{\phi_i}^2 v$, and thus $\widetilde{\mathcal{L}_{\mathrm{FP}}}$ takes the form of Eq. (3).

The eigensystem of the adjoint FP operator has a physically interesting implication. The adjoint FP equation (39) can formally be solved as

$$P_{\mathrm{FPT}}(\mathcal{N} \mid \boldsymbol{\phi}) = \exp[(\mathcal{N} - \epsilon)\mathcal{L}_{\mathrm{FP}}^{\dagger}]P_{\mathrm{FPT}}(\mathcal{N} = \epsilon \mid \boldsymbol{\phi}), \tag{47}$$

with a certain positive parameter ϵ. Expanding $P_{\mathrm{FPT}}(\mathcal{N} = \epsilon \mid \boldsymbol{\phi})$ by the eigensystem as[3]

$$P_{\mathrm{FPT}}(\mathcal{N} = \epsilon \mid \boldsymbol{\phi}) = \sum_n \alpha_n^{(\epsilon)}\tilde{\Psi}_n(\boldsymbol{\phi}) \tag{48}$$

leads to the solution

$$P_{\mathrm{FPT}}(\mathcal{N} \mid \boldsymbol{\phi}) = \sum_n \alpha_n^{(\epsilon)}\tilde{\Psi}_n(\boldsymbol{\phi})\mathrm{e}^{-\Lambda_n(\mathcal{N}-\epsilon)}. \tag{49}$$

One may take the limit $\epsilon \to 0$ as

$$P_{\mathrm{FPT}}(\mathcal{N} \mid \boldsymbol{\phi}) = \sum_n \alpha_n\tilde{\Psi}_n(\boldsymbol{\phi})\mathrm{e}^{-\Lambda_n\mathcal{N}}, \tag{50}$$

where $\alpha_n = \lim_{\epsilon\to 0}\alpha_n^{(\epsilon)}$. The functional form of Eq. (50) suggests that the PDF of $\mathcal{N}$ (and hence the primordial perturbation) has an exponentially heavy tail [63–65] in contrast to the naïve expectation that the physical perturbations are well described by the Gaussian distribution. In particular, the first eigenvalue, especially if it is of order unity, can exhibit a significant effect on the large-$\mathcal{N}$ (and hence large perturbation) probability and drastically change the abundance of astrophysical objects. This is why we want the method to calculate the first eigenvalue and the corresponding eigenfunction of the adjoint FP operator (or equivalently the Hermite FP operator $\widetilde{\mathcal{L}_{\mathrm{FP}}}$). However, this is a challenging computational task in classical computing, especially when the number of fields d is much larger than 1, and our quantum eigenvalue-finding algorithm proposed in Sec. III may be beneficial.

Let us briefly discuss the behavior of the Hermite FP operator before moving to specific examples. First, because $P_{\mathrm{FPT}}(\mathcal{N} > 0 \mid \boldsymbol{\phi} \in \partial\Omega) = 0$ by definition of $\mathcal{N}$ and $\partial\Omega$,[4] the boundary condition for the eigenfunctions is given by

$$\tilde{\Psi}_n(\boldsymbol{\phi} \in \partial\Omega) = 0 \;\Leftrightarrow\; \Psi_n(\boldsymbol{\phi} \in \partial\Omega) = 0. \tag{51}$$

In a single-field model, $d = 1$ (and ϕ denotes ϕ_1 for brevity), the eigenvalue equation (44) reduces to

$$\left(\partial_\phi^2 + \frac{v'}{v}\partial_\phi + \omega_n^2 \right)\Psi_n(\phi) = 0, \tag{52}$$

with

$$\omega_n^2 \simeq -\frac{1 - 2\Lambda_n\mathcal{P}_\zeta - 2\eta_{\mathrm{sto}}}{2M_{\mathrm{Pl}}^2 v\mathcal{P}_\zeta}. \tag{53}$$

Here, we define $\mathcal{P}_\zeta := 2v^3/(v'^2 M_{\mathrm{Pl}}^2) > 0$ and $\eta_{\mathrm{sto}} := v^2 v''/v'^2$, and we suppose $0 < v \ll 1$ for the inflation energy scale to be well below the Planck scale. $\mathcal{P}_\zeta$ is related to the amplitude of the curvature perturbation ζ in the perturbative evaluation. η_{sto} is called the *stochasticity parameter*, which indicates the magnitude of the stochastic correction to the perturbative evaluation [46]. It is decomposed as $\eta_{\mathrm{sto}} = \eta_V\mathcal{P}_\zeta/2$ where $\eta_V := M_{\mathrm{Pl}}^2 v''/v^2$ is known as the second slow-roll parameter and supposed to be small for single-field slow-roll inflation. Therefore, if the dynamics is well perturbative as $\mathcal{P}_\zeta \ll 1$, η_{sto} is also small, and then for $\Lambda_n \sim O(1)$, ω_n^2 becomes negative, which means that the eigenfunction is not normalizable. That is, unless the perturbativity is broken as $\mathcal{P}_\zeta \gtrsim 1$ in some region of the target space, $\widetilde{\mathcal{L}_{\mathrm{FP}}}$ have no order-unity eigenvalue, and thus there is no interesting physics caused by the large-$\mathcal{N}$ probability. Though this condition can be relaxed in multifield cases, the above discussion motivates us to seek the situation with $\mathcal{P}_\zeta \gtrsim 1$. Then, we below focus on models with a flat point $v' = 0$ at which $\mathcal{P}_\zeta$ can be divergent.

Although we would like to run our quantum algorithm for concrete problems including those with many fields, it is impossible today since there is no large-scale fault-tolerant quantum computer. Instead, to see if our method is promising for the eigenvalue problem in stochastic inflation, we take some classically (or even analytically) tractable cases with a few fields and check that we can take a test function $\tilde{f}_1$ overlapping with the true first eigenfunction well. With this condition satisfied, it is expected that our quantum algorithm finds the first eigenvalue efficiently. Specifically, expecting that the first eigenfunction has a simple functional shape with a single bump and no node in many cases, we take Gaussian test functions, which seem to work at least in the examined cases below.

A. Quantum well toy model

Let us first see the simplest single-field quantum well model as a toy example, reviewing Refs. [63,64]. As a zeroth order approximation of hilltop inflation [20,21], we suppose

---

[3]If the target space Ω is noncompact, the spectrum of the eigensystem is not discrete in general.

[4]$P_{\mathrm{FPT}}(\mathcal{N} \mid \boldsymbol{\phi} \in \partial\Omega) = \delta(\mathcal{N})$ according to the conservation of the probability.
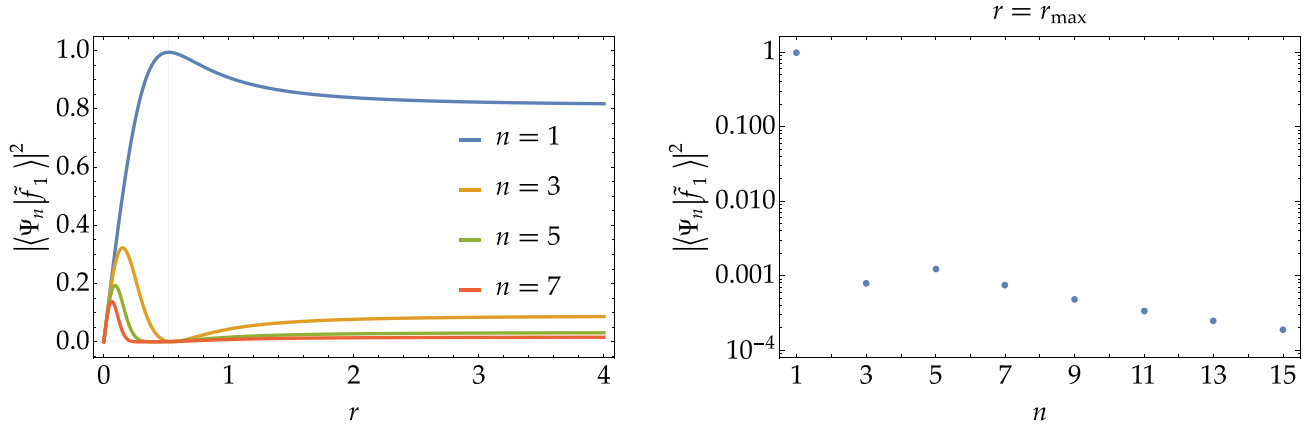
FIG. 1. Left: The absolute values squared of the inner product (58) as functions of the r parameter of the Gaussian test function $\tilde{f}_1$. The inner product of $n = 1$ is maximized at $r = r_{\max} \sim 0.52$ shown by the vertical thin line and reaches ~ 0.99. Right: The inner product for each n at $r = r_{\max}$.

that the inflaton potential has constant and compact support and is bounded by the absorbing (i.e., Dirichlet) boundaries:

$$v(\phi \in \Omega) = v_0, \quad \Omega = [-\phi_{\mathrm{f}}, \phi_{\mathrm{f}}], \quad \partial\Omega = \{-\phi_{\mathrm{f}}, \phi_{\mathrm{f}}\}, \quad (54)$$

where v_0 and ϕ_{f} are positive parameters. In this simplest setup, the normalized (i.e., $\langle \Psi_n | \Psi_m \rangle = \delta_{nm}$) eigenfunctions are easily obtained as

$$\Psi_n(\phi) = \frac{1}{\sqrt{\phi_{\mathrm{f}}}} \sin\left[n\pi \frac{\phi + \phi_{\mathrm{f}}}{2\phi_{\mathrm{f}}} \right], \quad n = 1, 2, 3, \ldots, \quad (55)$$

with the eigenvalues

$$\Lambda_n = \frac{n^2 \pi^2 M_{\mathrm{Pl}}^2 v_0}{4\phi_{\mathrm{f}}^2}. \quad (56)$$

If one chooses the normalized Gaussian

$$\tilde{f}_1(\phi) = \left(\sqrt{\pi} r \phi_{\mathrm{f}} \, \mathrm{erf}\left(\frac{1}{r} \right) \right)^{-1/2} \exp\left(-\frac{\phi^2}{2r^2\phi_{\mathrm{f}}^2} \right) \quad (57)$$

with a parameter $r > 0$ as the test function, its inner products with the eigenfunctions, which lead to the γ parameter in Eq. (29), are given by

$$\langle \tilde{f}_1 | \Psi_n \rangle \simeq \frac{\pi^{1/4} \sqrt{r}}{\sqrt{2} \, \mathrm{erf}(1/r)} e^{-\frac{\pi}{8}(4i(n-1)+n^2\pi r^2)}$$
$$\times \left(\mathrm{erf}\left(\frac{2 - in\pi r^2}{2\sqrt{2}r} \right) + \mathrm{erf}\left(\frac{2 + in\pi r^2}{2\sqrt{2}r} \right) \right) \quad (58)$$

for odd n or otherwise zero. $\mathrm{erf}(x) = (2/\sqrt{\pi}) \int_0^x e^{-t^2} dt$ is the error function. The r dependence of their absolute values squared is shown in the left panel of Fig. 1. The lowest state $n = 1$ dominates the higher modes, taking its maximal value ~ 0.99 at $r = r_{\max} \sim 0.52$ shown by the vertical thin line. The n dependence at $r = r_{\max}$ up to a higher value of n is exhibited in the right panel. One sees that the Gaussian test function can pick up the first eigenmode with the highest probability.

The flat inflection model (see, e.g., Refs. [66–69]) can also be simulated in the quantum well model just by changing the one boundary condition (we choose $\phi = \phi_{\mathrm{f}}$ without loss of generality) from the absorbing to the reflective (i.e., Neu-

mann) one. The eigenfunctions are then given by

$$\Psi_n(\phi) = \frac{1}{\sqrt{\phi_{\mathrm{f}}}} \sin\left[\left(n - \frac{1}{2} \right) \pi \frac{\phi + \phi_{\mathrm{f}}}{2\phi_{\mathrm{f}}} \right], \quad n = 1, 2, 3, \cdots, \quad (59)$$

with the eigenvalues

$$\Lambda_n = \frac{(n - 1/2)^2 \pi^2 M_{\mathrm{Pl}}^2 v_0}{4\phi_{\mathrm{f}}^2}. \quad (60)$$

Its inner product with the Gaussian test function

$$\tilde{f}_1(\phi) \simeq \left(\frac{\sqrt{\pi}}{2} r \phi_{\mathrm{f}} \, \mathrm{erf}\left(\frac{2}{r} \right) \right)^{-1} \exp\left(-\frac{(\phi - \phi_{\mathrm{f}})^2}{2r^2\phi_{\mathrm{f}}^2} \right) \quad (61)$$

reads

$$\langle \tilde{f}_1 | \Psi_n \rangle = -\frac{(-1)^n \pi^{1/4} \sqrt{r}}{2\sqrt{\mathrm{erf}(2/r)}} e^{-\frac{(2n-1)^2\pi^2 r^2}{32}}$$
$$\times \left(\mathrm{erf}\left(\frac{8 + (2n-1)i\pi r^2}{4\sqrt{2}r} \right) \right.$$
$$\left. + \mathrm{erf}\left(\frac{8 - (2n-1)i\pi r^2}{4\sqrt{2}r} \right) \right). \quad (62)$$

It is demonstrated in Fig. 2. The Gaussian test function can again pick up the lowest mode well.

Note that the reflective boundary is not compatible with our quantum algorithm. However, the eigenfunctions (59) are practically well reproduced by extending the calculation region slightly outside the quantum well, $\phi > \phi_{\mathrm{f}}$, with a steep ascent potential and imposing the absorbing boundary condition because ω_n^2 in Eq. (53) becomes negative for a steep potential and the eigenfunction rapidly damps outside the quantum well.

B. Hybrid inflation

Let us also see a two-field generalization called *hybrid inflation* [70]. There, the ϕ field rolls down along its potential $V_\phi(\phi)$ with the support potential of the so-called *waterfall*
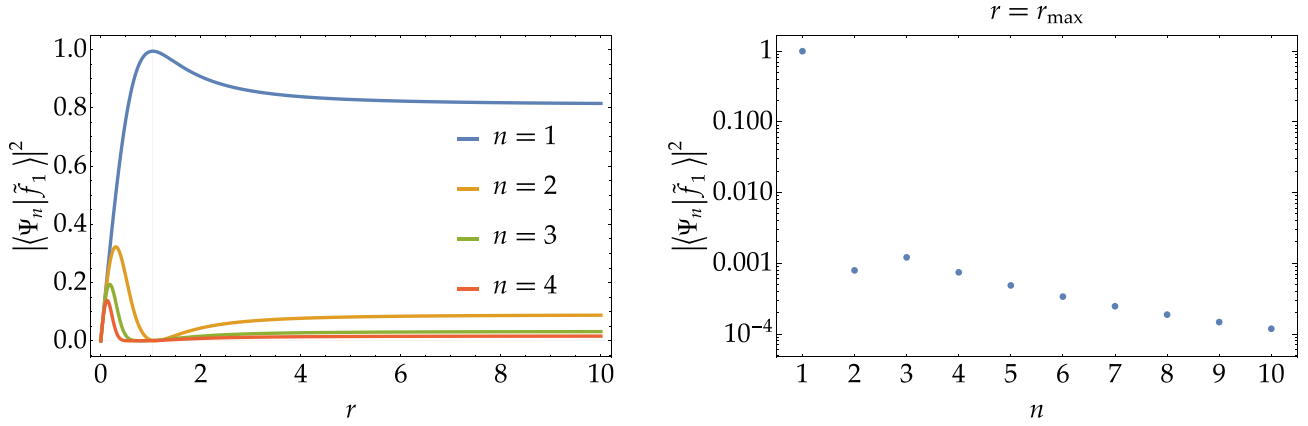
FIG. 2. The same plot as Fig. 1 but for the inner product (62) instead of (58). The vertical thin line in the left panel indicates $r = r_{\max} \simeq 1.04$ which maximizes the inner product for $n = 1$.

field ψ as

$$V(\phi, \psi) = V_\phi(\phi) + V_0 \left[\left(1 - \left(\frac{\psi}{M} \right)^2 \right) + 2 \left(\frac{\phi\psi}{\phi_c M} \right)^2 \right],$$
(63)

where V_0, M, and ϕ_c are the model parameters. Only positive values of ϕ are often considered and $V'_\phi(\phi)$ is chosen to be positive so ϕ rolls from a larger value to a smaller value. ψ is stabilized to $\psi = 0$ during $\phi > \phi_c$ due to the coupling with ϕ, while $\psi = 0$ is destabilized when $\phi < \phi_c$ and ψ rolls down to either potential minima $\psi = \pm M$. The ψ's fluctuations around $\phi = \phi_c$ determine which minima ψ falls to. The whole dynamics is hence stochastic, which makes the model nontrivial.

In the paper, we choose the inflaton potential to have a flat inflection:

$$V_\phi(\phi) = \frac{V_0 \beta}{M_{\rm Pl}^3} (\phi - \phi_c)^3,$$
(64)

with a parameter β, which not in hybrid inflation but as a single-field model, have been considered in a previous study [63]. Then, we numerically find the eigenvalues and eigenfunctions of $\widetilde{\mathcal{L}}_{\rm FP}$, adopting the following parameter values:

$$V_0 = 10^{-15} M_{\rm Pl}^4, \quad M = 10^{16}\,{\rm GeV}, \quad \phi_c = \sqrt{2}M, \quad \beta = 10^4.$$
(65)

We take the rectangular absorbing boundary.[5] $[\phi_{\min}, \phi_{\max}]$, the range of ϕ, is set so that $|\phi - \phi_c|/M_{\rm Pl} \leqslant \beta^{-1/3}$, following Ref. [63]. $\psi_{\min}$ and $\psi_{\max}$, the endpoints of ψ, are set so that at the points, the second slow-roll parameter $M_{\rm Pl}^2 |\partial_\psi^2 v/v|$ for ψ is 1, which means that the inflation ends, with $\phi = \phi_c$. It is important to sufficiently resolve the region near the inflection point, where the stochasticity is significant. Thus, in ϕ, we set 1000 equally spaced grid points in $[\phi_{{\rm sto},-}, \phi_{{\rm sto},+}]$

---

[5]Although the reflective condition is usually set on the high-potential side, whether we set the absorbing or reflective condition has almost no effect on the low eigenvalues and eigenfunctions because of the steep potential away from the inflection point, as mentioned in Sec. IV A.

and 500 points each in $[\phi_{\min}, \phi_{{\rm sto},-}]$ and $[\phi_{{\rm sto},+}, \phi_{\max}]$ so that $\log |\phi - \phi_c|$ is equally spaced. Here, $\phi_{{\rm sto},+}$ is the value of $\phi > \phi_c$ at which the stochasticity parameter $\eta_{{\rm sto},\phi}$ for ϕ becomes 0.1 with $\psi = 0$ and $\phi_{{\rm sto},-} = \phi_c - (\phi_{{\rm sto},+} - \phi_c)$. Similarly, in ψ, we set 1000 equally spaced grid points in $[\psi_{{\rm sto},-}, \psi_{{\rm sto},+}]$, and 500 points each in $[\psi_{\min}, \psi_{{\rm sto},-}]$ and $[\psi_{{\rm sto},+}, \psi_{\max}]$ so that $\log |\psi|$ is equally spaced, where $\psi_{{\rm sto},+} > 0$ is set so that $\eta_{{\rm sto},\psi} = 0.1$ at $(\phi, \psi) = (\phi_{{\rm sto},+}, \psi_{{\rm sto},+})$ and $\psi_{{\rm sto},-} = -\psi_{{\rm sto},+}$. Although such grid points that are not equally spaced in linear scale do not match the setting in our quantum algorithm, it does not matter for our current objective to see the overlap between the test function and the eigenfunctions: It is calculated as

$$\frac{\left| \sum_{k,l} \tilde{f}_1 \left(\phi_k^{\rm gr}, \psi_l^{\rm gr} \right) \Psi_n \left(\phi_k^{\rm gr}, \psi_l^{\rm gr} \right) \Delta\phi_k \Delta\psi_l \right|^2}{\sum_{k,l} \left| \tilde{f}_1 \left(\phi_k^{\rm gr}, \psi_l^{\rm gr} \right) \right|^2 \Delta\phi_k \Delta\psi_l \times \sum_{k,l} \left| \Psi_n \left(\phi_k^{\rm gr}, \psi_l^{\rm gr} \right) \right|^2 \Delta\phi_k \Delta\psi_l},$$
(66)

where $\phi_k^{\rm gr}$ (respectively, $\psi_l^{\rm gr}$) is the kth grid point in ϕ (respectively, ψ) and $\Delta\phi_k = \phi_{k+1}^{\rm gr} - \phi_k^{\rm gr}$ and $\Delta\psi_k = \psi_{k+1}^{\rm gr} - \psi_k^{\rm gr}$. We will consider extending our quantum algorithm so that nonequidistant grid points can be dealt with in future works.

By using `eigs` in SciPy [71], we find the first ten eigenvalues and eigenfunctions, which are shown in Figs. 3 and 4, respectively. Noting that the eigenfunctions have peaks in the
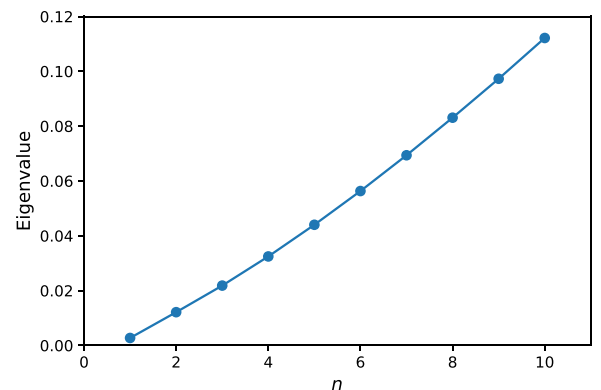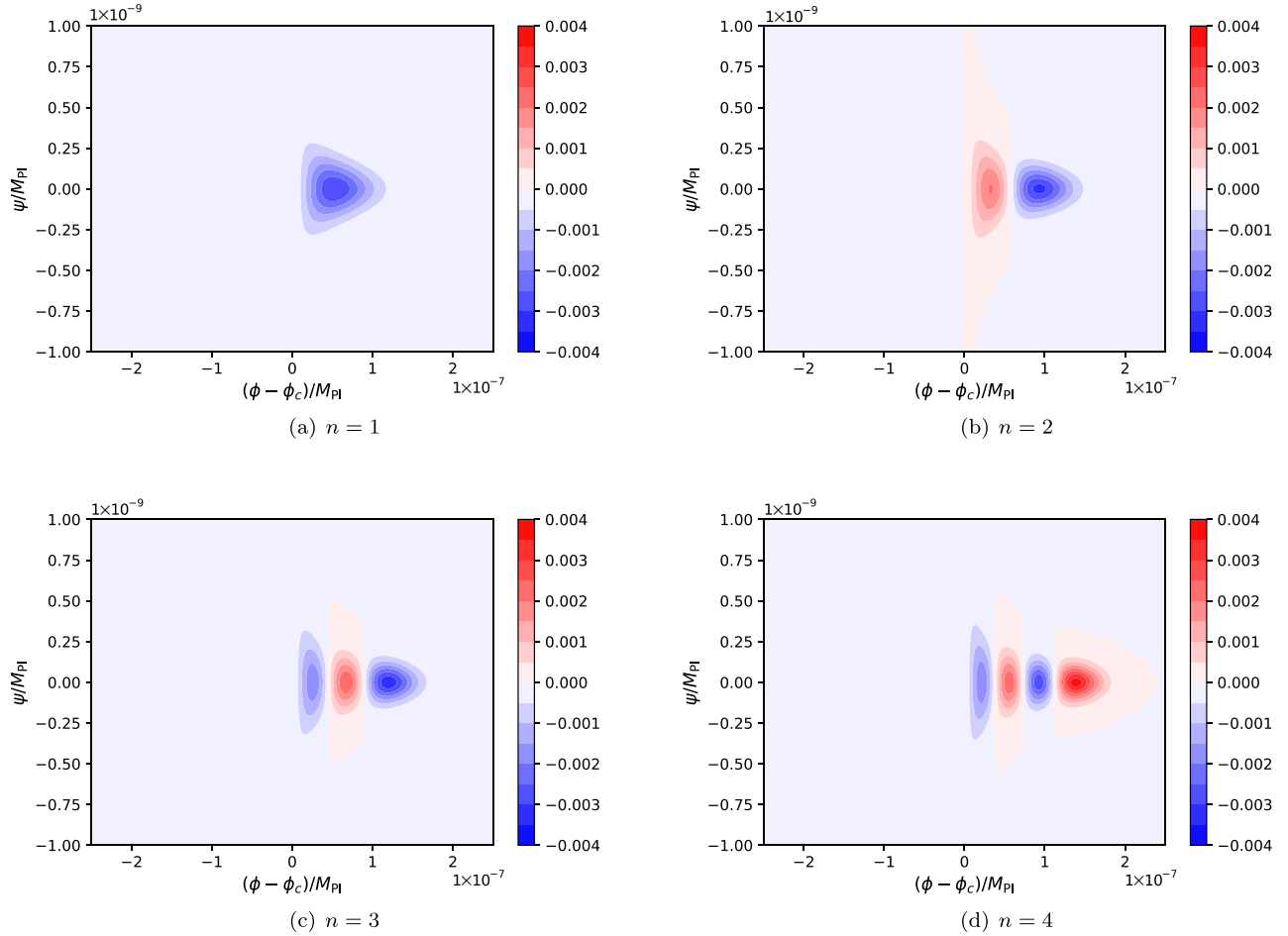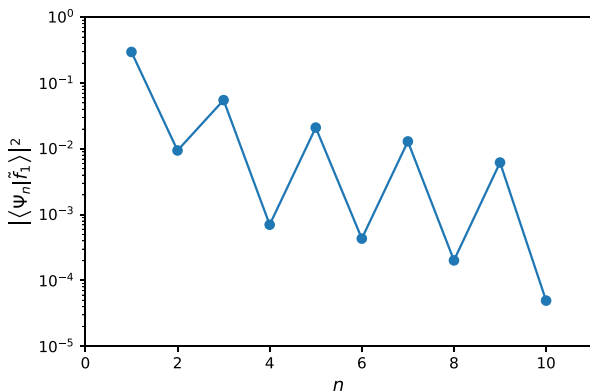

FIG. 3. The first ten eigenvalues of $\widetilde{\mathcal{L}}_{\rm FP}$ with V in Eqs. (63) and (64) for the parameters in Eq. (65).

FIG. 4. The first four eigenfunctions of the same $\widetilde{\mathcal{L}_{\mathrm{FP}}}$ as Fig. 3.

high-stochasticity region, we take the following Gaussian test function:

$$\tilde{f}_1(\phi, \psi) \propto \exp\left(-\frac{(\phi - \phi_{\mathrm{c}})^2}{2(\phi_{\mathrm{sto},+} - \phi_{\mathrm{c}})^2} - \frac{\psi^2}{2\psi_{\mathrm{sto},+}^2}\right). \quad (67)$$

The overlaps between this and the eigenfunctions are shown in Fig. 5. One sees that the overlap is significant for the first

FIG. 5. The squared inner products between the quantum states encoding the Gaussian test function $\tilde{f}_1$ in Eq. (67) and those encoding nth eigenfunctions of the same $\widetilde{\mathcal{L}_{\mathrm{FP}}}$ as Fig. 3.

eigenfunction, which implies that with this test function, our quantum algorithm will also work well in this model.

V. SUMMARY

In this paper, we considered a quantum algorithm for calculating the first eigenvalue of differential operators. Under the finite difference approximation of a given operator, this problem boils down to the matrix eigenvalue problem, but in multidimensional cases it is computationally demanding because of the exponential increase of the size of the approximating matrix. Then, we proposed a quantum algorithm for this task, leveraging the QSVT-based quantum algorithm for finding the first eigenvalue of matrices in Ref. [9]. Our quantum algorithm has the query complexity scaling as $\widetilde{O}(1/\epsilon^2)$ on the accuracy ϵ in the eigenvalue, which shows the improvement compared to the existing quantum algorithm for the same task with complexity of order $\widetilde{O}(1/\epsilon^3)$.

As a potential application target for our algorithm, we considered a problem in cosmology, finding the eigenvalue of the adjoint FP operator $\mathcal{L}_{\mathrm{FP}}^\dagger$ in stochastic inflation, which is related to the tail shape of the PDF of the primordial perturbation. Although we cannot run our algorithm for concrete instances of this problem now because of the absence of large-scale fault-tolerant quantum computers, we conducted numerical demonstrations for some problem instances in

shochastic inflation to show that our method is promising. We take Gaussian functions as test functions, expecting the first eigenfunctions to have a single-bump shape, and saw that they in fact overlap with the first eigenfunctions well in the considered problems, which implies that one of the conditions for our method to work would be satisfied.

Nevertheless, refining the way to set the test function should be considered in future works, since it is not obvious that the current approach will also work in more complicated problems, such as higher-dimensional ones. Preparing the test function is an issue also in ground energy estimation in condensed matter physics and chemistry, where various approaches have been proposed: e.g., the adiabatic state preparation considered in Ref. [72]. It will be interesting and significant to explore applications of such advanced state preparation methods to differential operator eigenproblems, learning from existing studies in other fields.

APPENDIX: PROOFS

1. Proof of Theorem 1

Before the proof, we introduce some kinds of norms and smoothness classes of functions. Let $\Omega \subset \mathbb{R}^d$ be a bounded region. For a function $g : \Omega \to \mathbb{R}$, we define

$$|g|_{0,\Omega} := \sup_{\mathbf{x} \in \Omega} |g(\mathbf{x})| \tag{A1}$$

and

$$|g|_{a,\Omega} := \sum_{|\boldsymbol{\alpha}| \leqslant \lceil a \rceil - 1} |D^{\boldsymbol{\alpha}} g(\mathbf{x})|_{0,\Omega}$$
$$+ \sum_{|\boldsymbol{\alpha}| = \lceil a \rceil - 1} \sup_{\mathbf{x}, \mathbf{y} \in \Omega} \frac{|D^{\boldsymbol{\alpha}} g(\mathbf{x}) - D^{\boldsymbol{\alpha}} g(\mathbf{y})|}{\|\mathbf{x} - \mathbf{y}\|^{a - \lceil a \rceil + 1}}, \tag{A2}$$

with $a \in \mathbb{R}_+$. We say that $g \in C^a(\overline{\Omega})$ if $|g|_{a,\Omega} < \infty$ and that $g \in C^a(\Omega)$ if $g \in C^a(\overline{O})$ for every $\overline{O} \subset \Omega$. Obviously, any function in $C^a(\overline{\Omega})$ needs to be $(\lceil a \rceil - 1)$-times differentiable. We can easily see that any $\lceil a \rceil$ times continuously differentiable function on $\overline{\Omega}$ is in $C^a(\overline{\Omega}) \cap C^a(\Omega)$.

Then, the proof of Theorem 1 is as follows.

Proof of Theorem 1. Theorem 1 is obtained by just applying Theorem 5.1 in Ref. [33] to Problem 1 with the finite difference approximation in Eq. (9). Now, we just check that the conditions for applying Theorem 6.4 in Ref. [33] are satisfied.

(1) $L_{n_{\mathrm{gr}}}$ acts locally, that is, any entry $(L_{n_{\mathrm{gr}}})_{\mathbf{j}_1,\mathbf{j}_2}$ corresponding to the grid points $\mathbf{x}_{\mathbf{j}_1}^{\mathrm{gr}}$ and $\mathbf{x}_{\mathbf{j}_2}^{\mathrm{gr}}$ such that $\|\mathbf{x}_{\mathbf{j}_1}^{\mathrm{gr}} - \mathbf{x}_{\mathbf{j}_2}^{\mathrm{gr}}\| > h$ is 0.

(2) $L_{n_{\mathrm{gr}}}$ is symmetric.

(3) Condition (i) (see Ref. [33] for details; the same applies below).

In the grid point set $\mathcal{D}_{n_{\mathrm{gr}}}$ given in Sec. II B, for any adjacent point pair $(\mathbf{x}_{\mathbf{j}_1}^{\mathrm{gr}}, \mathbf{x}_{\mathbf{j}_2}^{\mathrm{gr}})$, where $\mathbf{j}_1 = \mathbf{j}_2 \pm \mathbf{e}_i$ for some $i \in [d]$, the

corresponding entry $(L_{n_{\mathrm{gr}}})_{\mathbf{j}_1,\mathbf{j}_2}$ in $L_{n_{\mathrm{gr}}}$ is nonzero. Besides, for any $\mathbf{x}_{\mathbf{j}}^{\mathrm{gr}}, \mathbf{x}_{\mathbf{j}'}^{\mathrm{gr}} \in \mathcal{D}_{n_{\mathrm{gr}}}$, we can move from $\mathbf{x}_{\mathbf{j}}^{\mathrm{gr}}$ to $\mathbf{x}_{\mathbf{j}'}^{\mathrm{gr}}$ by some sequence of transitions to an adjacent point. Combining these observations, we see that the condition (i) is satisfied.

(4) Condition (ii).

We have

$$\sum_{\substack{\mathbf{j}' \in \mathcal{D}_{n_{\mathrm{gr}}} \\ \mathbf{j}' \neq \mathbf{j}}} \left| h^2 (L_{n_{\mathrm{gr}}})_{\mathbf{j},\mathbf{j}'} \right| \leqslant 2d a_{\max},$$

$$\frac{1}{h^2 \left| (L_{n_{\mathrm{gr}}})_{\mathbf{j},\mathbf{j}} \right|} \leqslant \frac{1}{2d a_{\min}}, \tag{A3}$$

$$\sum_{\substack{\mathbf{j}' \in \mathcal{D}_{n_{\mathrm{gr}}} \\ \mathbf{j}' \neq \mathbf{j}}} \left| \frac{(L_{n_{\mathrm{gr}}})_{\mathbf{j},\mathbf{j}'}}{(L_{n_{\mathrm{gr}}})_{\mathbf{j},\mathbf{j}}} \right| \leqslant 1$$

for any $\mathbf{j} \in [n_{\mathrm{gr}}]_0^d$, where $a_{\min} := \min_{\substack{i \in [d] \\ \mathbf{x} \in \overline{\mathcal{D}}}} a_i(\mathbf{x})$. This means that condition (ii) is satisfied,[6]

(5) Condition (iii).

It is obvious that $\sum_{\substack{\mathbf{j}' \in \mathcal{D}_{n_{\mathrm{gr}}} \\ \mathbf{j}' \neq \mathbf{j}}} |(L_{n_{\mathrm{gr}}})_{\mathbf{j},\mathbf{j}'}| \leqslant (L_{n_{\mathrm{gr}}})_{\mathbf{j},\mathbf{j}}$ for any $\mathbf{j} := [n_{\mathrm{gr}}]_0^d$, which means that the first part of this condition is satisfied. The second part is irrelevant in the current case, since now $\mathcal{D}_{n_{\mathrm{gr}}}^* := \mathcal{D}_{n_{\mathrm{gr}}} - \mathcal{D}'_{n_{\mathrm{gr}}}$ is empty.[7] Here, $\mathcal{D}'_{n_{\mathrm{gr}}} := \{\mathbf{x} \in \mathcal{D}_{n_{\mathrm{gr}}} \mid \inf_{\mathbf{x}' \in \partial \mathcal{D}} \|\mathbf{x} - \mathbf{x}'\| \geqslant h\}$, which is now equal to $\mathcal{D}_{n_{\mathrm{gr}}}$.

(6) Condition (iv).

This is also irrelevant in the current case since $\mathcal{D}_{n_{\mathrm{gr}}}^* = \emptyset$.

(7) Condition (v).

It is obvious that $(L_{n_{\mathrm{gr}}})_{\mathbf{j},\mathbf{j}'} \leqslant 0$ for any $\mathbf{j}, \mathbf{j}' \in [n_{\mathrm{gr}}]_0^d$ such that $\mathbf{j} \neq \mathbf{j}'$, which means this condition is satisfied.

(8) Let us check that, in the words of Ref. [33] , $L_{n_{\mathrm{gr}}}$ is consistent of order 2 with $\mathcal{L}$ in $\mathcal{D}_{n_{\mathrm{gr}}}$, that is, there exists a constant C independent of h such that

$$\left| \mathcal{L} f(\mathbf{x}_{\mathbf{j}}^{\mathrm{gr}}) - (L_{n_{\mathrm{gr}}} \mathbf{v}_{f,n_{\mathrm{gr}}})_{\mathbf{j}} \right| \leqslant C h^{\mu} |f|_{\mu+2, S_{h,\mathbf{j}} \cap \mathcal{D}} \tag{A4}$$

holds for any $\mu \in (0, 2]$, $\mathbf{j} \in [n_{\mathrm{gr}}]_0^d$ and $f \in C^{\mu+2}(\overline{S_{h,\mathbf{j}} \cap \mathcal{D}})$. Here, $S_{h,\mathbf{j}} := \{\mathbf{x} \in \mathbb{R}^d \mid \|\mathbf{x} - \mathbf{x}_{\mathbf{j}}^{\mathrm{gr}}\| < h\}$ is the sphere of radius h centered at $\mathbf{x}_{\mathbf{j}}^{\mathrm{gr}}$. $f \in C^{\mu+2}(\overline{S_{h,\mathbf{j}} \cap \mathcal{D}})$ implies the following. First, f is $\tilde{\mu}$ times differentiable, where $\tilde{\mu} = \lceil \mu + 2 \rceil - 1$ and, thus, as we can see using Taylor's theorem,

$$f(\mathbf{x}_{\mathbf{j}}^{\mathrm{gr}} + \delta \mathbf{e}_i) = \sum_{n=0}^{\tilde{\mu}-1} \frac{1}{n!} \frac{\partial^n f}{\partial x_i^n}(\mathbf{x}_{\mathbf{j}}^{\mathrm{gr}}) \delta^n + \frac{1}{\tilde{\mu}!} \frac{\partial^{\tilde{\mu}} f}{\partial x_i^{\tilde{\mu}}}(\mathbf{x}_{\mathbf{j}}^{\mathrm{gr}} + \delta' \mathbf{e}_i) \delta^{\tilde{\mu}} \tag{A5}$$

---

[6]Note that, in our definition, $L_{n_{\mathrm{gr}}}$ has no entry corresponding to a point in $\partial \mathcal{D}$. Even if we make it have such entries as in Ref. [33], they are zero because of the Dirichlet boundary condition and thus have nothing to do with the condition (ii).

[7]Note the differences of the notations in this paper and Ref. [33]. $\mathcal{D}'_{n_{\mathrm{gr}}}$ and $\mathcal{D}_{n_{\mathrm{gr}}}^*$ correspond to Ω'_h and Ω_h^* in Ref. [33], respectively.

holds for any $\mathbf{j} \in [n_{\mathrm{gr}}]_0^d$, $i \in [d]$, and $\delta \in [-h, h]$, with some real number δ' that is between 0 and δ and dependent on i, $\mathbf{x}_{\mathbf{j}}^{\mathrm{gr}}$ and δ. Second, for any $\mathbf{x}, \mathbf{y} \in S_{h,\mathbf{j}} \cap \mathcal{D}$ and $i \in [d]$,

$$\left| \frac{\partial^{\tilde{\mu}} f}{\partial x_i^{\tilde{\mu}}}(\mathbf{x}) - \frac{\partial^{\tilde{\mu}} f}{\partial x_i^{\tilde{\mu}}}(\mathbf{y}) \right| \leqslant |f|_{\mu+2, S_{h,\mathbf{j}} \cap \mathcal{D}} \|\mathbf{x} - \mathbf{y}\|^{\mu+2-\lceil \mu+2 \rceil+1} \tag{A6}$$

holds. Combining Eqs. (A5) and (A6), we have

$$f(\mathbf{x}_{\mathbf{j}}^{\mathrm{gr}} + \delta \mathbf{e}_i) = \sum_{n=0}^{\tilde{\mu}} \frac{1}{n!} \frac{\partial^n f}{\partial x_i^n}(\mathbf{x}_{\mathbf{j}}^{\mathrm{gr}}) \delta^n + R, \tag{A7}$$

with the residual term R bounded as

$$|R| \leqslant \frac{1}{\tilde{\mu}!} |f|_{\mu+2, S_{h,\mathbf{j}} \cap \mathcal{D}} |\delta|^{\mu+2}. \tag{A8}$$

For a_i, since it is four times continuously differentiable on $\mathcal{D}$ and $\tilde{\mu} \leqslant 3$, Taylor's theorem implies that, for any $n \in [\tilde{\mu}]$,

$$a_i(\mathbf{x}_{\mathbf{j}}^{\mathrm{gr}} + \delta \mathbf{e}_i) = \sum_{m=0}^{n} \frac{1}{m!} \frac{\partial^m a_i}{\partial x_i^m}(\mathbf{x}_{\mathbf{j}}^{\mathrm{gr}}) \delta^m + \frac{1}{(n+1)!} \frac{\partial^{n+1} a_i}{\partial x_i^{n+1}}(\mathbf{x}_{\mathbf{j}}^{\mathrm{gr}} + \delta'' \mathbf{e}_i) \delta^{n+1} \tag{A9}$$

holds with some real number δ'' that is between 0 and δ and dependent on i, n, $\mathbf{x}_{\mathbf{j}}^{\mathrm{gr}}$ and δ. By using Eqs. (A7) and (A9) with $\delta = \pm h$ and $\delta = \pm \frac{h}{2}$ in Eq. (10), we obtain

$$\left(L_{n_{\mathrm{gr}}} \mathbf{v}_{f, n_{\mathrm{gr}}} \right)_{\mathbf{j}} = \sum_{i=1}^{d} \left(\frac{\partial a_i}{\partial x_i}(\mathbf{x}_{\mathbf{j}}^{\mathrm{gr}}) \frac{\partial f}{\partial x_i}(\mathbf{x}_{\mathbf{j}}^{\mathrm{gr}}) + a_i(\mathbf{x}_{\mathbf{j}}^{\mathrm{gr}}) \frac{\partial^2 f}{\partial x_i^2}(\mathbf{x}_{\mathbf{j}}^{\mathrm{gr}}) \right) + a_0(\mathbf{x}_{\mathbf{j}}^{\mathrm{gr}}) f(\mathbf{x}_{\mathbf{j}}^{\mathrm{gr}}) + R'. \tag{A10}$$

Here, the residual term R' is bounded as

$$|R'| \leqslant \sum_{i=1}^{d} \sum_{n=0}^{\tilde{\mu}} \frac{1}{2^{\tilde{\mu}-n} (\tilde{\mu} - n + 1)! n!} a_{\max}^{(\tilde{\mu}-n+1)} \left| \frac{\partial^n f}{\partial x_i^n} \right|_{0, S_{h,\mathbf{j}} \cap \mathcal{D}} h^{\tilde{\mu}-1} + \frac{2d}{\tilde{\mu}!} |f|_{\mu+2, S_{h,\mathbf{j}} \cap \mathcal{D}} h^\mu, \tag{A11}$$

where, for $n \in \mathbb{N}$, $a_{\max}^{(n)} := \max_{i \in [d]} |\frac{\partial^n a_i}{\partial x_i^n}|_{0, \mathcal{D}}$. This implies that Eq. (A4) holds with C

$$C := \max_{n \in [\tilde{\mu}+1]_0} \frac{a_{\max}^{(\tilde{\mu}-n+1)}}{2^{\tilde{\mu}-n} (\tilde{\mu} - n + 1)! n!} \times (U - L)^{\lceil \mu+2 \rceil - \mu - 2} + \frac{2d}{\tilde{\mu}!}. \tag{A12}$$

(9) Lastly, let us check that the each eigenfunction f_k of $\mathcal{L}$ is in $C^4(\overline{\mathcal{D}})$. Since $a_0, \ldots, a_d$ are now four times continuously differentiable and thus twice continuously differentiable, they are in $C^2(\overline{\mathcal{D}}) \cap C^2(\mathcal{D})$. Then, Theorem 6.3 in [33] implies that f_k is in $C^4(\overline{\mathcal{D}}) \cap C^4(\mathcal{D})$. ∎

2. Proof of Corollary 1

Proof of Corollary 1. Note that, given $(\alpha, a, 0)$-block encoding U_H of H, the quantum algorithm in Ref. [9] relies on a unitary PROJ $(\mu, \frac{\epsilon}{2\alpha}, \epsilon')$ constructed with U_H, where $\mu \in \mathbb{R}$ is any real number, ϵ' is set to $\epsilon' = \gamma/2$, and

$$\left\| (\langle 0|^{\otimes(a+3)} \otimes I_{2^n}) \mathrm{PROJ}\left(\mu, \frac{\epsilon}{2\alpha}, \epsilon' \right) |0\rangle^{\otimes(a+3)} |\phi_1\rangle \right\| \begin{cases} \geqslant \gamma - \frac{\epsilon'}{2}; & \text{if } \lambda_1 \leqslant \mu - \epsilon \\ \leqslant \frac{\epsilon'}{2}; & \text{if } \lambda_1 \geqslant \mu + \epsilon \end{cases} \tag{A13}$$

holds. U_H is used only in this unitary and, thus, if we can construct a unitary $\widetilde{\mathrm{PROJ}}(\mu, \frac{\epsilon}{2\alpha}, \epsilon')$ that has the same property as Eq. (A13) using O_{row}^H, O_{col}^H, and O_{ent}^H instead of U_H, we can run the quantum algorithm replacing $\mathrm{PROJ}(\mu, \frac{\epsilon}{2\alpha}, \epsilon')$ with $\widetilde{\mathrm{PROJ}}(\mu, \frac{\epsilon}{2\alpha}, \epsilon')$. In particular, it suffices that we have $\widetilde{\mathrm{PROJ}}(\mu, \frac{\epsilon}{2\alpha}, \epsilon')$ such that

$$\left\| (\langle 0|^{\otimes(a+3)} \otimes I_{2^n}) \widetilde{\mathrm{PROJ}}\left(\mu, \frac{\epsilon}{2\alpha}, \epsilon' \right) (|0\rangle^{\otimes(a+3)} \otimes I_{2^n}) - (\langle 0|^{\otimes(a+3)} \otimes I_{2^n}) \mathrm{PROJ}\left(\mu, \frac{\epsilon}{2\alpha}, \frac{\epsilon'}{2} \right) (|0\rangle^{\otimes(a+3)} \otimes I_{2^n}) \right\| \leqslant \frac{\epsilon'}{4}, \tag{A14}$$

which, as we can see by simple algebra, leads to $\widetilde{\mathrm{PROJ}}(\mu, \frac{\epsilon}{2\alpha}, \epsilon')$ satisfying the property like Eq. (A13).

Then, let us consider how to construct such $\widetilde{\mathrm{PROJ}}(\mu, \frac{\epsilon}{2\alpha}, \epsilon')$, fixing α to $\tilde{\alpha} := s\|H\|_{\max}$ and a to $\tilde{a} := n + 3$. On the one hand, we note that

$$\mathrm{PROJ}\left(\mu, \frac{\epsilon}{2\tilde{\alpha}}, \frac{\epsilon'}{2} \right) = (\mathrm{Had} \otimes I_{2^{n+\tilde{a}+3}}) \otimes \left(|0\rangle \langle 0| \otimes I_{2^{n+\tilde{a}+3}} + |1\rangle \langle 1| \otimes \mathrm{REF}\left(\mu, \frac{\epsilon}{2\tilde{\alpha}}, \frac{\epsilon'}{2} \right) \right) \otimes (\mathrm{Had} \otimes I_{2^{n+\tilde{a}+3}}) \tag{A15}$$

by the definition in Ref. [9]. Here, Had is a Hadamard gate and $\mathrm{REF}(\mu, \frac{\epsilon}{2\tilde{\alpha}}, \frac{\epsilon'}{2})$ is a $(\tilde{\alpha}, \tilde{a} + 2, 0)$-block-encoding of $-S(\frac{H-\mu I}{\tilde{\alpha}+|\mu|}; \frac{\epsilon}{2\tilde{\alpha}}, \frac{\epsilon'}{2})$ with $S(\cdot; \frac{\epsilon}{2\tilde{\alpha}}, \frac{\epsilon'}{2})$ being some polynomial of degree $d_{\tilde{\alpha}, \epsilon, \epsilon'} = O(\frac{\tilde{\alpha}}{\epsilon} \log(\frac{1}{\epsilon'}))$ (see [9] for the details). On the other hand, because of Theorem 2, we can construct a $(\tilde{\alpha}, \tilde{a}, \tilde{\epsilon})$-block-encoding $\tilde{U}_H$ of H with O_{row}^H, O_{col}^H, and O_{ent}^H, where

$$\tilde{\epsilon} := \left(\frac{\epsilon'}{8 d_{\tilde{\alpha}, \epsilon, \epsilon'}} \right)^2 \tilde{\alpha}. \tag{A16}$$

$\tilde{U}_H$ can be regarded as a $(\tilde{\alpha}, \tilde{a}, 0)$-block encoding of some matrix $\tilde{H} \in \mathbb{C}^{2^n \times 2^n}$ such that $\|\tilde{H} - H\| \leqslant \tilde{\epsilon}$. Thus, because of Lemma 22 in the full version of Ref. [7], replacing U_H in $\mathrm{REF}(\mu, \frac{\epsilon}{2\tilde{\alpha}}, \frac{\epsilon'}{2})$ with $\tilde{U}_H$ yields a $(\tilde{\alpha}, \tilde{a}+2, 0)$-block encoding $\widetilde{\mathrm{REF}}$ of $\tilde{S} \in \mathbb{C}^{2^n \times 2^n}$ such that

$$\left\| \tilde{S} - \left(-S\left(\frac{H-\mu I}{\tilde{\alpha}+|\mu|}; \frac{\epsilon}{2\tilde{\alpha}}, \frac{\epsilon'}{2} \right) \right) \right\| \leqslant 4 d_{\tilde{\alpha}, \epsilon, \epsilon'} \sqrt{\left\| \frac{H-\mu I}{\tilde{\alpha}+|\mu|} - \frac{\tilde{H} - \mu I}{\tilde{\alpha}+|\mu|} \right\|} \leqslant \frac{4 d_{\tilde{\alpha}, \epsilon, \epsilon'}}{\sqrt{\tilde{\alpha}}} \sqrt{\|H - \tilde{H}\|} \leqslant \frac{\epsilon'}{2}. \tag{A17}$$

Consequently, replacing U_H in $\mathrm{PROJ}(\mu, \frac{\epsilon}{2\tilde{\alpha}}, \frac{\epsilon'}{2})$ with $\tilde{U}_H$ yields $\widetilde{\mathrm{PROJ}}(\mu, \frac{\epsilon}{2\tilde{\alpha}}, \frac{\epsilon'}{2})$, satisfying

$$\left\| (\langle 0|^{\otimes(\tilde{a}+3)} \otimes I_{2^n}) \widetilde{\mathrm{PROJ}}\left(\mu, \frac{\epsilon}{2\alpha}, \epsilon' \right) (|0\rangle^{\otimes(\tilde{a}+3)} \otimes I_{2^n}) - (\langle 0|^{\otimes(\tilde{a}+3)} \otimes I_{2^n}) \mathrm{PROJ}\left(\mu, \frac{\epsilon}{2\alpha}, \frac{\epsilon'}{2} \right) (|0\rangle^{\otimes(\tilde{a}+3)} \otimes I_{2^n}) \right\|$$

$$= \left\| (\langle +| \langle 0|^{\tilde{a}+2} \otimes I_{2^n}) \left(|1\rangle \langle 1| \otimes \left(\widetilde{\mathrm{REF}} - \mathrm{REF}\left(\mu, \frac{\epsilon}{2\tilde{\alpha}}, \frac{\epsilon'}{2} \right) \right) \right) (|+\rangle |0\rangle^{\otimes(\tilde{a}+2)} \otimes I_{2^n}) \right\|$$

$$= \frac{1}{2} \left\| (\langle 0|^{\tilde{a}+2} \otimes I_{2^n}) \left(\widetilde{\mathrm{REF}} - \mathrm{REF}\left(\mu, \frac{\epsilon}{2\tilde{\alpha}}, \frac{\epsilon'}{2} \right) \right) (|0\rangle^{\otimes(\tilde{a}+2)} \otimes I_{2^n}) \right\|$$

$$= \frac{1}{2} \left\| \tilde{S} - \left(-S\left(\frac{H-\mu I}{\tilde{\alpha}+|\mu|}; \frac{\epsilon}{2\tilde{\alpha}}, \frac{\epsilon'}{2} \right) \right) \right\| \leqslant \frac{\epsilon'}{4}, \tag{A18}$$

namely, Eq. (A14). Here, at the first equality, we have used Eq. (A15) and the similar relationship between $\widetilde{\mathrm{PROJ}}(\mu, \frac{\epsilon}{2\alpha}, \frac{\epsilon'}{2})$ and $\widetilde{\mathrm{REF}}$.

Lastly, let us evaluate the number of uses of $O_{\mathrm{row}}^H, O_{\mathrm{col}}^H, O_{\mathrm{ent}}^H$ and elementary gates and the number of qubits in the quantum algorithm. As said above, we replace $\mathrm{PROJ}(\mu, \frac{\epsilon}{2\alpha}, \epsilon')$ in the original algorithm in Ref. [9] with $\widetilde{\mathrm{PROJ}}(\mu, \frac{\epsilon}{2\alpha}, \epsilon')$, which is yielded by replacing U_H in $\mathrm{PROJ}(\mu, \frac{\epsilon}{2\alpha}, \frac{\epsilon'}{2})$ with $\tilde{U}_H$. If we use U_H, the number of calls to it, the number of uses of other one- and two-qubit gates, and the number of qubits in $\mathrm{PROJ}(\mu, \frac{\epsilon}{2\alpha}, \epsilon')$ and $\mathrm{PROJ}(\mu, \frac{\epsilon}{2\alpha}, \frac{\epsilon'}{2})$ are of the same order. Since we use $O_{\mathrm{row}}^H, O_{\mathrm{col}}^H$, and O_{ent}^H in $\tilde{U}_H$ only $O(1)$ times, we get the evaluation (23) on the number of queries to these by simply replacing α in Eq. (19) with $\tilde{\alpha}$. In $\tilde{U}_H$, we use $O(n + \log^{5/2}(\frac{s^2 \|H\|_{\max}}{\tilde{\epsilon}}))$ additional one- and two-qubit gates, and multiplying this evaluation by the number of queries to $\tilde{U}_H$ and adding Eq. (21) yields the total gate number evaluation in Eq. (25). $O(\log^{5/2}(\frac{s^2 \|H\|_{\max}}{\tilde{\epsilon}}))$ ancilla qubits are used in $\tilde{U}_H$, and summing up this and Eq. (22) with $a = \tilde{a}$ yields the total qubit number evaluation in Eq. (26). Since $U_{|\phi_0\rangle}$ is outside $\widetilde{\mathrm{PROJ}}(\mu, \frac{\epsilon}{2\alpha}, \epsilon')$, we get the evaluation (24) on the number of queries to this by simply replacing α in Eq. (20) with $\tilde{\alpha}$. ∎

3. Proof of Theorem 4

Before presenting the rest of the proof, we give some lemmas.

Lemma A 1. Let $\mathbf{u} = (u_0, \ldots, u_{N_{\mathrm{gr}}-1}), \mathbf{v} = (v_0, \ldots, v_{N_{\mathrm{gr}}-1}) \in \mathbb{R}^{N_{\mathrm{gr}}}$. Suppose that $\|\mathbf{v}_{n_{\mathrm{gr}}}\|_{n_{\mathrm{gr}}} = 1$ and that $\|\mathbf{u} - \mathbf{v}\|_{\max} \leqslant \epsilon$ with some $\epsilon \in \mathbb{R}$. Then,

$$\langle \mathbf{u} | \mathbf{v} \rangle \geqslant 1 - 2(U - L)^{d/2} \epsilon. \tag{A19}$$

Proof. $\|\mathbf{u} - \mathbf{v}\|_{\max} \leqslant \epsilon$ implies that

$$u_i - \epsilon \leqslant v_i \leqslant u_i + \epsilon \tag{A20}$$

for each $i \in [N_{\mathrm{gr}}]_0$, and that

$$\|\mathbf{u}\| \geqslant \|\mathbf{v}\| - \|\mathbf{u} - \mathbf{v}\| \geqslant \|\mathbf{v}\| - \sqrt{N_{\mathrm{gr}}} \epsilon. \tag{A21}$$

In addition, the Cauchy-Schwarz inequality implies that

$$\sum_{i=0}^{N_{\mathrm{gr}}-1} |u_i| \leqslant \sqrt{N_{\mathrm{gr}}} \|\mathbf{u}\|. \tag{A22}$$

Furthermore, by the definition of $\| \cdot \|_{n_{\mathrm{gr}}}$,

$$h^{d/2} \|\mathbf{v}\| = \|\mathbf{v}\|_{n_{\mathrm{gr}}} = 1 \tag{A23}$$

holds. Combining these, we have

$$\begin{aligned}
\langle \mathbf{u} | \mathbf{v} \rangle &= \frac{\sum_{i=0}^{N_{\mathrm{gr}}-1} u_i v_i}{\|\mathbf{u}\| \|\mathbf{v}\|} \\
&\geqslant \frac{\sum_{i=0}^{N_{\mathrm{gr}}-1} u_i (u_i - \mathrm{sgn}(u_i) \times \epsilon)}{\|\mathbf{u}\| \|\mathbf{v}\|} \\
&= \frac{\|\mathbf{u}\|}{\|\mathbf{v}\|} - \epsilon \frac{\sum_{i=0}^{N_{\mathrm{gr}}-1} |u_i|}{\|\mathbf{u}\| \|\mathbf{v}\|} \\
&\geqslant 1 - \frac{2\sqrt{N_{\mathrm{gr}}} \epsilon}{\|\mathbf{v}\|} \\
&\geqslant 1 - 2(U - L)^{d/2} \epsilon, \tag{A24}
\end{aligned}$$

where we use Eq. (A20) at the first inequality, Eqs. (A21) and (A22) at the second inequality, and Eq. (A23) at the last equality. ∎

ALGORITHM 2. J^{-1}.

Input: $K \in [N_{\mathrm{gr}}]_0$
Output: $k_1, \ldots, k_d$ such that $K = \sum_{i=1}^{d} n_{\mathrm{gr}}^{i-1} k_i$
   1: Set $K_d = K$.
   2: **for** $i = d, \ldots, 2$ **do**
   3:     Divide K_i by n_{gr}^{i-1}, and let the quotient and remainder be k_i and K_{i-1}, respectively.
   4: **end for**
   5: Divide K_1 by n_{gr}, and let the quotient and remainder be k_2 and k_1, respectively.

Lemma A 2. Let $|\phi\rangle, |\psi\rangle, |\zeta\rangle$ be quantum states on an n_{gr}-qubit register. Suppose that $|\langle\phi|\psi\rangle| \geqslant \gamma$ for $\gamma \in (0, 1)$. Then, $|\langle\phi|\zeta\rangle| \geqslant \frac{\gamma}{2}$ holds if

$$|\langle\psi|\zeta\rangle| \geqslant \eta(\gamma). \tag{A25}$$

Proof. We can write

$$|\phi\rangle = \alpha |\psi\rangle + \beta |\psi_\perp\rangle \tag{A26}$$

with $\alpha, \beta \in \mathbb{C}$ such that $|\alpha| \geqslant \gamma$ and $|\beta| \leqslant \sqrt{1 - \gamma^2}$, and a quantum state $|\psi_\perp\rangle$ orthogonal to $|\psi\rangle$. Besides, Eq. (A25) implies that

$$|\langle\zeta|\psi_\perp\rangle| \leqslant \sqrt{1 - \eta^2(\gamma)}. \tag{A27}$$

Then, we have

$$|\langle\phi|\zeta\rangle| \geqslant |\alpha| \times |\langle\zeta|\psi\rangle| - |\beta| \times |\langle\zeta|\psi_\perp\rangle| \geqslant \gamma\eta(\gamma) - \sqrt{1 - \gamma^2}\sqrt{1 - \eta^2(\gamma)}. \tag{A28}$$

By some algebra, we see that the last line is greater than or equal to $\frac{\gamma}{2}$. ∎

Then, the rest of the proof of Theorem 4 is as follows.

Rest of the proof of Theorem 4.

How to construct $O_{\mathrm{row}}^{L_{n_{\mathrm{gr}}}}, O_{\mathrm{col}}^{L_{n_{\mathrm{gr}}}}$, and $O_{\mathrm{ent}}^{L_{n_{\mathrm{gr}}}}$.

Let us start from $O_{\mathrm{row}}^{L_{n_{\mathrm{gr}}}}$. For $L_{n_{\mathrm{gr}}}$, whose sparsity is $2d + 1$, r_{ik} is given as[8]

$$r_{ik} = J(J^{-1}(i) + \mathbf{d}_{i,k}). \tag{A29}$$

Here, $\mathbf{d}_{i,k} \in \mathbb{R}^d$ is defined as

$$\mathbf{d}_{i,k} = \begin{cases} -\mathbf{e}_k & \text{if } k = 1, \ldots, d \\ \mathbf{0} & \text{if } k = d + 1 \\ \mathbf{e}_{k-d-1} & \text{if } k = d + 2, \ldots, 2d + 1, \end{cases} \tag{A30}$$

where $\mathbf{0}$ is the d-dimensional zero vector. $J : [n_{\mathrm{gr}}]_0^d \to [N_{\mathrm{gr}}]_0$ is the map in Eq. (6), which is implemented by some additions and multiplications. J^{-1} is its inverse, which is implemented by a sequence of divisions shown in Algorithm 2. Therefore, we see that we can implement $O_{\mathrm{row}}^{L_{n_{\mathrm{gr}}}}$ using $O(d)$ arithmetic circuits.

$O_{\mathrm{col}}^{L_{n_{\mathrm{gr}}}}$ is implemented similarly.

Next, let us consider the implementation of $O_{\mathrm{ent}}^{L_{n_{\mathrm{gr}}}}$. For $K, K' \in [N_{\mathrm{gr}}]_0$, we can perform the following operation:

$$|K\rangle |K'\rangle |0\rangle^{\otimes(4d+5)}$$

$$\to |K\rangle |K'\rangle |\mathbf{k}\rangle_{\mathrm{bin}} |\mathbf{k}'\rangle_{\mathrm{bin}} |0\rangle^{\otimes(4d+3)}$$

$$\to |K\rangle |K'\rangle |\mathbf{k}\rangle_{\mathrm{bin}} |\mathbf{k}'\rangle_{\mathrm{bin}} |a_0(\mathbf{x}_\mathbf{k}^{\mathrm{gr}})\rangle \left|a_1\left(\mathbf{x}_\mathbf{k}^{\mathrm{gr}} + \frac{h}{2}\mathbf{e}_1\right)\right\rangle \left|a_1\left(\mathbf{x}_\mathbf{k}^{\mathrm{gr}} - \frac{h}{2}\mathbf{e}_1\right)\right\rangle \cdots \left|a_d\left(\mathbf{x}_\mathbf{k}^{\mathrm{gr}} + \frac{h}{2}\mathbf{e}_d\right)\right\rangle \left|a_d\left(\mathbf{x}_\mathbf{k}^{\mathrm{gr}} - \frac{h}{2}\mathbf{e}_d\right)\right\rangle \otimes |0\rangle^{\otimes(2d+2)}$$

$$\to |K\rangle |K'\rangle |\mathbf{k}\rangle_{\mathrm{bin}} |\mathbf{k}'\rangle_{\mathrm{bin}} |a_0(\mathbf{x}_\mathbf{k}^{\mathrm{gr}})\rangle \left|a_1\left(\mathbf{x}_\mathbf{k}^{\mathrm{gr}} + \frac{h}{2}\mathbf{e}_1\right)\right\rangle \left|a_1\left(\mathbf{x}_\mathbf{k}^{\mathrm{gr}} - \frac{h}{2}\mathbf{e}_1\right)\right\rangle \cdots \left|a_d\left(\mathbf{x}_\mathbf{k}^{\mathrm{gr}} + \frac{h}{2}\mathbf{e}_d\right)\right\rangle \left|a_d\left(\mathbf{x}_\mathbf{k}^{\mathrm{gr}} - \frac{h}{2}\mathbf{e}_d\right)\right\rangle$$

$$\otimes |1_{\mathbf{k}'-\mathbf{k}=\mathbf{0}}\rangle |1_{\mathbf{k}'-\mathbf{k}=\mathbf{e}_1}\rangle |1_{\mathbf{k}'-\mathbf{k}=-\mathbf{e}_1}\rangle \cdots |1_{\mathbf{k}'-\mathbf{k}=\mathbf{e}_d}\rangle |1_{\mathbf{k}'-\mathbf{k}=-\mathbf{e}_d}\rangle |0\rangle$$

$$= |K\rangle |K'\rangle |\mathbf{k}\rangle_{\mathrm{bin}} |\mathbf{k}'\rangle_{\mathrm{bin}} |a_0(\mathbf{x}_\mathbf{k}^{\mathrm{gr}})\rangle \left|a_1\left(\mathbf{x}_\mathbf{k}^{\mathrm{gr}} + \frac{h}{2}\mathbf{e}_1\right)\right\rangle \left|a_1\left(\mathbf{x}_\mathbf{k}^{\mathrm{gr}} - \frac{h}{2}\mathbf{e}_1\right)\right\rangle \cdots \left|a_d\left(\mathbf{x}_\mathbf{k}^{\mathrm{gr}} + \frac{h}{2}\mathbf{e}_d\right)\right\rangle \left|a_d\left(\mathbf{x}_\mathbf{k}^{\mathrm{gr}} - \frac{h}{2}\mathbf{e}_d\right)\right\rangle$$

---

[8]Strictly speaking, this expression for r_{ik} holds for only i such that none of the entries of $\sigma^{-1}(i)$ is 0 or $n_{\mathrm{gr}} - 1$, and otherwise the expression is slightly modified. However, such a handling is straightforward and thus we do not show the complete expression here for conciseness.

$$\otimes \left(1_{\mathbf{k'}-\mathbf{k}\neq\mathbf{0},\pm\mathbf{e}_1,\dots,\pm\mathbf{e}_d} |0\rangle^{\otimes(2d+1)} |0\rangle + 1_{\mathbf{k'}-\mathbf{k}=\mathbf{0}} |1\rangle |0\rangle^{\otimes 2d} |0\rangle \right.$$

$$+ 1_{\mathbf{k'}-\mathbf{k}=\mathbf{e}_1} |0\rangle |1\rangle |0\rangle |0\rangle^{\otimes(2d-2)} |0\rangle + 1_{\mathbf{k'}-\mathbf{k}=-\mathbf{e}_1} |0\rangle |0\rangle |1\rangle |0\rangle^{\otimes(2d-2)} |0\rangle + \cdots$$

$$\left. + 1_{\mathbf{k'}-\mathbf{k}=\mathbf{e}_d} |0\rangle |0\rangle^{\otimes(2d-2)} |1\rangle |0\rangle |0\rangle + 1_{\mathbf{k'}-\mathbf{k}=-\mathbf{e}_d} |0\rangle |0\rangle^{\otimes(2d-2)} |0\rangle |1\rangle |0\rangle \right)$$

$$\rightarrow |K\rangle |K'\rangle |\mathbf{k}\rangle_{\text{bin}} |\mathbf{k'}\rangle_{\text{bin}} \left|a_0(\mathbf{x}_{\mathbf{k}}^{\text{gr}})\right\rangle \left|a_1\left(\mathbf{x}_{\mathbf{k}}^{\text{gr}}+\frac{h}{2}\mathbf{e}_1\right)\right\rangle \left|a_1\left(\mathbf{x}_{\mathbf{k}}^{\text{gr}}-\frac{h}{2}\mathbf{e}_1\right)\right\rangle \cdots \left|a_d\left(\mathbf{x}_{\mathbf{k}}^{\text{gr}}+\frac{h}{2}\mathbf{e}_d\right)\right\rangle \left|a_d\left(\mathbf{x}_{\mathbf{k}}^{\text{gr}}-\frac{h}{2}\mathbf{e}_d\right)\right\rangle$$

$$\otimes \left(1_{\mathbf{k'}-\mathbf{k}\neq\mathbf{0},\pm\mathbf{e}_1,\dots,\pm\mathbf{e}_d} |0\rangle^{\otimes(2d+1)} |0\rangle + 1_{\mathbf{k'}-\mathbf{k}=\mathbf{0}} |1\rangle |0\rangle^{\otimes 2d} \left|(L_{n_{\text{gr}}})_{K,K'}\right\rangle \right.$$

$$+ 1_{\mathbf{k'}-\mathbf{k}=\mathbf{e}_1} |0\rangle |1\rangle |0\rangle |0\rangle^{\otimes(2d-2)} \left|(L_{n_{\text{gr}}})_{K,K'}\right\rangle + 1_{\mathbf{k'}-\mathbf{k}=-\mathbf{e}_1} |0\rangle |0\rangle |1\rangle |0\rangle^{\otimes(2d-2)} \left|(L_{n_{\text{gr}}})_{K,K'}\right\rangle + \cdots$$

$$\left. + 1_{\mathbf{k'}-\mathbf{k}=\mathbf{e}_d} |0\rangle |0\rangle^{\otimes(2d-2)} |1\rangle |0\rangle \left|(L_{n_{\text{gr}}})_{K,K'}\right\rangle + 1_{\mathbf{k'}-\mathbf{k}=-\mathbf{e}_d} |0\rangle |0\rangle^{\otimes(2d-2)} |0\rangle |1\rangle \left|(L_{n_{\text{gr}}})_{K,K'}\right\rangle \right)$$

$$= |K\rangle |K'\rangle |\mathbf{k}\rangle_{\text{bin}} |\mathbf{k'}\rangle_{\text{bin}} \left|a_0(\mathbf{x}_{\mathbf{k}}^{\text{gr}})\right\rangle \left|a_1\left(\mathbf{x}_{\mathbf{k}}^{\text{gr}}+\frac{h}{2}\mathbf{e}_1\right)\right\rangle \left|a_1\left(\mathbf{x}_{\mathbf{k}}^{\text{gr}}-\frac{h}{2}\mathbf{e}_1\right)\right\rangle \cdots \left|a_d\left(\mathbf{x}_{\mathbf{k}}^{\text{gr}}+\frac{h}{2}\mathbf{e}_d\right)\right\rangle \left|a_d\left(\mathbf{x}_{\mathbf{k}}^{\text{gr}}-\frac{h}{2}\mathbf{e}_d\right)\right\rangle$$

$$\otimes \left|1_{\mathbf{k'}-\mathbf{k}=\mathbf{0}}\right\rangle \left|1_{\mathbf{k'}-\mathbf{k}=\mathbf{e}_1}\right\rangle \left|1_{\mathbf{k'}-\mathbf{k}=-\mathbf{e}_1}\right\rangle \cdots \left|1_{\mathbf{k'}-\mathbf{k}=\mathbf{e}_d}\right\rangle \left|1_{\mathbf{k'}-\mathbf{k}=-\mathbf{e}_d}\right\rangle \left|(L_{n_{\text{gr}}})_{K,K'}\right\rangle$$

$$\rightarrow |K\rangle |K'\rangle |0\rangle^{\otimes(4d+5)} \left|(L_{n_{\text{gr}}})_{K,K'}\right\rangle. \tag{A31}$$

Here, the transformation at the first arrow is done by the circuit for J^{-1}, where $\mathbf{k} = J^{-1}(K)$ and $\mathbf{k'} = J^{-1}(K')$. At the second arrow, we make $O(d)$ uses of $O_{a_0}, \dots, O_{a_d}$. At the third arrow, we use $O(d)$ arithmetic circuits, and at the fourth arrow we use controlled versions of arithmetic circuits to compute the entries of $L_{n_{\text{gr}}}$ with the values of $a_0, \dots, a_d$ computed in the previous step according to Eq. (9). The last arrow in Eq. (A31) is uncomputation of the first and second ones. Note that the circuit for the operation in Eq. (A31) is nothing but $O_{\text{ent}}^{L_{n_{\text{gr}}}}$.

Lastly, let us count the number of the queries to $O_{a_0}, \dots, O_{a_d}$ and arithmetic circuits in $O_{\text{row}}^{L_{n_{\text{gr}}}}$, $O_{\text{col}}^{L_{n_{\text{gr}}}}$, and $O_{\text{ent}}^{L_{n_{\text{gr}}}}$. In $O_{\text{row}}^{L_{n_{\text{gr}}}}$ and $O_{\text{col}}^{L_{n_{\text{gr}}}}$, we use $O(d)$ arithmetic circuits. In $O_{\text{ent}}^{L_{n_{\text{gr}}}}$, we make $O(d)$ uses of $O_{a_0}, \dots, O_{a_d}$ and (controlled) arithmetic circuits.

Accuracy

Because of Theorem 1, for n_{gr} in (32), $\lambda_{n_{\text{gr}}}^1$ is $\frac{\epsilon}{2}$-close to λ_1. Besides, the output of $\mathsf{EstEig}(L_{n_{\text{gr}}}, \frac{\epsilon}{2}, \delta)$ is a $\frac{\epsilon}{2}$-approximation of $\lambda_{n_{\text{gr}}}^1$. Therefore, the output of Algorithm 1 is an ϵ approximation of λ_1.

Query complexity

The sparsity of $L_{n_{\text{gr}}}$ is

$$s = O(d). \tag{A32}$$

Its max norm is bounded as

$$\|L_{n_{\text{gr}}}\|_{\max} \leqslant \frac{2d a_{\max}}{h^2} + a_{0,\max} = O\left(\frac{d a_{\max}}{(U-L)^2} \times \max\left\{ \frac{C_{\mathcal{L}}^1}{\epsilon}, \frac{D_{\mathcal{L}}^1 (U-L)^{\frac{d}{2}}}{1-\eta(\gamma)} \right\} + a_{0,\max} \right) \tag{A33}$$

for n_{gr} in Eq. (32).

Let us evaluate the overlap between $|\mathbf{v}_{\tilde{f}_1, n_{\text{gr}}}\rangle$ and $|\mathbf{v}_{n_{\text{gr}}}^1\rangle$. Because of Theorem 1,

$$\left\|\mathbf{v}_{n_{\text{gr}}}^1 - \mathbf{v}_{f_1, n_{\text{gr}}}\right\|_{\max} \leqslant \frac{1-\eta(\gamma)}{2(U-L)^{d/2}} \tag{A34}$$

holds for n_{gr} in Eq. (32). Because of Lemma A 1, this leads to

$$\left|\langle \mathbf{v}_{n_{\text{gr}}}^1 | \mathbf{v}_{f_1, n_{\text{gr}}} \rangle\right| \geqslant \eta(\gamma). \tag{A35}$$

Then, because of Lemma A 2, combining this and Eq. (29) leads to

$$\left|\langle \mathbf{v}_{n_{\text{gr}}}^1 | \mathbf{v}_{\tilde{f}_1, n_{\text{gr}}} \rangle\right| \geqslant \frac{\gamma}{2}. \tag{A36}$$

Let us incorporate the above observations into Corollary 1. By using Eqs. (A32) and (A33) in Eqs. (23) and (24) and replacing γ with $\frac{\gamma}{2}$, we obtain estimations of the numbers of queries to $O_{\text{row}}^{L_{n_{\text{gr}}}}$, $O_{\text{col}}^{L_{n_{\text{gr}}}}$, $O_{\text{ent}}^{L_{n_{\text{gr}}}}$, and $O_{\tilde{f}_1, n_{\text{gr}}}$ in $\mathsf{EstEig}(L_{n_{\text{gr}}}, \frac{\epsilon}{2}, \delta)$ in Algorithm 1, and, noting that $O_{\text{row}}^{L_{n_{\text{gr}}}}$, $O_{\text{col}}^{L_{n_{\text{gr}}}}$, and $O_{\text{ent}}^{L_{n_{\text{gr}}}}$ consist of $O(d)$ uses of $O_{a_0}, \dots, O_{a_d}$ and arithmetic circuits, we get the query complexity estimations in Eqs. (30) and (31). ∎

[1] S. Larsson and V. Thomée, *Partial Differential Equations with Numerical Methods* (Springer, Berlin, 2003), Vol. 45.

[2] J. W. Demmel, *Applied Numerical Linear Algebra* (Society for Industrial and Applied Mathematics, Philadelphia, 1997).

[3] A. W. Harrow, A. Hassidim, and S. Lloyd, Quantum algorithm for linear systems of equations, Phys. Rev. Lett. **103**, 150502 (2009).

[4] D. S. Abrams and S. Lloyd, Quantum algorithm providing exponential speed increase for finding eigenvalues and eigenvectors, Phys. Rev. Lett. **83**, 5162 (1999).

[5] I. Kerenidis and A. Prakash, Quantum recommendation systems, in *8th Innovations in Theoretical Computer Science Conference (ITCS 2017)* (Schloss Dagstuhl–Leibniz-Zentrum für Informatik, Dagstuhl, Germany, 2017), Vol. 67, pp. 49:1–49:21.

[6] S. Chakraborty, A. Gilyén, and S. Jeffery, The Power of Block-Encoded Matrix Powers: Improved regression techniques via faster Hamiltonian simulation, in *46th International Colloquium on Automata, Languages, and Programming (ICALP 2019)* (Schloss Dagstuhl–Leibniz-Zentrum für Informatik, Dagstuhl, Germany, 2019), Vol. 132, pp. 33:1–33:14.

[7] A. Gilyén, Y. Su, G. H. Low, and N. Wiebe, Quantum singular value transformation and beyond: Exponential improvements for quantum matrix arithmetics, in *Proceedings of the 51st Annual ACM SIGACT Symposium on Theory of Computing (STOC 2019)* (Association for Computing Machinery, New York, 2019), pp. 193–204, arXiv:1806.01838.

[8] Y. Ge, J. Tura, and J. I. Cirac, Faster ground state preparation and high-precision ground energy estimation with fewer qubits, J. Math. Phys. **60**, 022202 (2019).

[9] L. Lin and Y. Tong, Near-optimal ground state preparation, Quantum **4**, 372 (2020).

[10] J. M. Martyn, Z. M. Rossi, A. K. Tan, and I. L. Chuang, Grand unification of quantum algorithms, PRX Quantum **2**, 040203 (2021).

[11] G. H. Low and Y. Su, Quantum eigenvalue processing, in *Proceedings of the 65th IEEE Symposium on Foundations of Computer Science (FOCS 2024)* (IEEE Computer Society, Washington, DC, 2024), pp. 1051–1062.

[12] T. Szkopek, V. Roychowdhury, E. Yablonovitch, and D. S. Abrams, Eigenvalue estimation of differential operators with a quantum algorithm, Phys. Rev. A **72**, 062318 (2005).

[13] A. Papageorgiou and H. Woźniakowski, Classical and quantum complexity of the Sturm–Liouville eigenvalue problem, Quantum Info. Proc. **4**, 87 (2005).

[14] A. J. Bessen, A lower bound for the Sturm–Liouville eigenvalue problem on a quantum computer, J. Complexity **22**, 660 (2006).

[15] G. H. Low and I. L. Chuang, Optimal Hamiltonian simulation by quantum signal processing, Phys. Rev. Lett. **118**, 010501 (2017).

[16] G. H. Low and I. L. Chuang, Hamiltonian simulation by qubitization, Quantum **3**, 163 (2019).

[17] A. A. Starobinsky, A new type of isotropic cosmological models without singularity, Phys. Lett. B **91**, 99 (1980).

[18] K. Sato, First-order phase transition of a vacuum and the expansion of the Universe, Mon. Not. R. Astron. Soc. **195**, 467 (1981).

[19] A. H. Guth, The inflationary universe: A possible solution to the horizon and flatness problems, Phys. Rev. D **23**, 347 (1981).

[20] A. D. Linde, A new inflationary universe scenario: A possible solution of the horizon, flatness, homogeneity, isotropy and primordial monopole problems, Phys. Lett. B **108**, 389 (1982).

[21] A. Albrecht and P. J. Steinhardt, Cosmology for grand unified theories with radiatively induced symmetry breaking, Phys. Rev. Lett. **48**, 1220 (1982).

[22] A. D. Linde, Chaotic inflation, Phys. Lett. B **129**, 177 (1983).

[23] A. A. Starobinsky, Dynamics of phase transition in the new inflationary universe scenario and generation of perturbations, Phys. Lett. B **117**, 175 (1982).

[24] A. A. Starobinsky, Stochastic de sitter (inflationary) stage in the early universe, Lect. Notes Phys. **246**, 107 (1986).

[25] Y. Nambu and M. Sasaki, Stochastic stage of an inflationary universe model, Phys. Lett. B **205**, 441 (1988).

[26] Y. Nambu and M. Sasaki, Stochastic approach to chaotic inflation and the distribution of universes, Phys. Lett. B **219**, 240 (1989).

[27] H. E. Kandrup, Stochastic inflation as a time dependent random walk, Phys. Rev. D **39**, 2245 (1989).

[28] K.-i. Nakao, Y. Nambu, and M. Sasaki, Stochastic dynamics of new inflation, Prog. Theor. Phys. **80**, 1041 (1988).

[29] Y. Nambu, Stochastic dynamics of an inflationary model and initial distribution of universes, Prog. Theor. Phys. **81**, 1037 (1989).

[30] S. Mollerach, S. Matarrese, A. Ortolan, and F. Lucchin, Stochastic inflation in a simple two field model, Phys. Rev. D **44**, 1670 (1991).

[31] A. D. Linde, D. A. Linde, and A. Mezhlumian, From the big bang theory to the theory of a stationary universe, Phys. Rev. D **49**, 1783 (1994).

[32] A. A. Starobinsky and J. Yokoyama, Equilibrium state of a selfinteracting scalar field in the De Sitter background, Phys. Rev. D **50**, 6357 (1994).

[33] J. R. Kuttler, Finite difference approximations for eigenvalues of uniformly elliptic operators, SIAM J. Numer. Anal. **7**, 206 (1970).

[34] E. Muñoz-Coreas and H. Thapliyal, Everything you always wanted to know about quantum circuits, in *Wiley Encyclopedia of Electrical and Electronics Engineering* (John Wiley & Sons, Ltd., New York, 2022), pp. 1–17.

[35] T. Häner, M. Roetteler, and K. M. Svore, Optimizing quantum circuits for arithmetic, arXiv:1805.12445.

[36] L. Grover and T. Rudolph, Creating superpositions that correspond to efficiently integrable probability distributions, arXiv:quant-ph/0208112.

[37] Y. R. Sanders, G. H. Low, A. Scherer, and D. W. Berry, Black-box quantum state preparation without arithmetic, Phys. Rev. Lett. **122**, 020502 (2019).

[38] C. Zoufal, A. Lucchi, and S. Woerner, Quantum generative adversarial networks for learning and loading random distributions, npj Quantum Inf. **5**, 103 (2019).

[39] A. Holmes and A. Y. Matsuura, Efficient quantum circuits for accurate state preparation of smooth, differentiable functions, in *2020 IEEE International Conference on Quantum Computing and Engineering (QCE)* (IEEE Computer Society, Washington, DC, 2020), pp. 169–179.

[40] A. G. Rattew and B. Koczor, Preparing arbitrary continuous functions in quantum registers with logarithmic complexity, arXiv:2205.00519.

[41] S. McArdle, A. Gilyén, and M. Berta, Quantum state preparation without coherent arithmetic, arXiv:2210.14892.

[42] G. Marin-Sanchez, J. Gonzalez-Conde, and M. Sanz, Quantum algorithms for approximate function loading, Phys. Rev. Res. **5**, 033114 (2023).

[43] M. Moosa, T. W. Watts, Y. Chen, A. Sarma, and P. L. McMahon, Linear-depth quantum circuits for loading Fourier approximations of arbitrary functions, Quantum Sci. Technol. **9**, 015002 (2024).

[44] Y. Akrami *et al.* (Planck Collaboration), Planck 2018 results. X. Constraints on inflation, Astron. Astrophys. **641**, A10 (2020).

[45] D. Cruces, Review on stochastic approach to inflation, Universe **8**, 334 (2022).

[46] V. Vennin and A. A. Starobinsky, Correlation functions in stochastic inflation, Eur. Phys. J. C **75**, 413 (2015).

[47] J. Tokuda and T. Tanaka, Statistical nature of infrared dynamics on de Sitter background, J. Cosmol. Astropart. Phys. **02**, 014, (2018).

[48] J. Tokuda and T. Tanaka, Can all the infrared secular growth really be understood as increase of classical statistical variance? J. Cosmol. Astropart. Phys. **11**, 022 (2018).

[49] L. Pinol, S. Renaux-Petel, and Y. Tada, Inflationary stochastic anomalies, Class. Quantum Grav. **36**, 07LT01 (2019).

[50] L. Pinol, S. Renaux-Petel, and Y. Tada, A manifestly covariant theory of multifield stochastic inflation in phase space: Solving the discretisation ambiguity in stochastic inflation, J. Cosmol. Astropart. Phys. 04 (2021) 048.

[51] A. A. Starobinsky, Multicomponent de sitter (inflationary) stages and the generation of perturbations, JETP Lett. **42**, 152 (1985).

[52] D. S. Salopek and J. R. Bond, Nonlinear evolution of long wavelength metric fluctuations in inflationary models, Phys. Rev. D **42**, 3936 (1990).

[53] M. Sasaki and E. D. Stewart, A General analytic formula for the spectral index of the density perturbations produced during inflation, Prog. Theor. Phys. **95**, 71 (1996).

[54] M. Sasaki and T. Tanaka, Superhorizon scale dynamics of multiscalar inflation, Prog. Theor. Phys. **99**, 763 (1998).

[55] D. Wands, K. A. Malik, D. H. Lyth, and A. R. Liddle, A new approach to the evolution of cosmological perturbations on large scales, Phys. Rev. D **62**, 043527 (2000).

[56] D. H. Lyth, K. A. Malik, and M. Sasaki, A general proof of the conservation of the curvature perturbation, J. Cosmol. Astropart. Phys. **05**, 004 (2005).

[57] D. H. Lyth and Y. Rodriguez, The inflationary prediction for primordial non-Gaussianity, Phys. Rev. Lett. **95**, 121302 (2005).

[58] T. Fujita, M. Kawasaki, Y. Tada, and T. Takesako, A new algorithm for calculating the curvature perturbations in stochastic inflation, J. Cosmol. Astropart. Phys. 12 (2013) 036.

[59] T. Fujita, M. Kawasaki, and Y. Tada, Non-perturbative approach for curvature perturbations in stochastic δN formalism, J. Cosmol. Astropart. Phys. 10 (2014) 030.

[60] K. Ando and V. Vennin, Power spectrum in stochastic inflation, J. Cosmol. Astropart. Phys. 04 (2021) 057.

[61] Y. Tada and V. Vennin, Statistics of coarse-grained cosmological fields in stochastic inflation, J. Cosmol. Astropart. Phys. 02 (2022) 021.

[62] C. Animali and V. Vennin, Clustering of primordial black holes from quantum diffusion during inflation, J. Cosmol. Astropart. Phys. 08 (2024) 026.

[63] J. M. Ezquiaga, J. García-Bellido, and V. Vennin, The exponential tail of inflationary fluctuations: Consequences for primordial black holes, J. Cosmol. Astropart. Phys. 03 (2020) 029.

[64] C. Pattison, V. Vennin, H. Assadullahi, and D. Wands, Quantum diffusion during inflation and primordial black holes, J. Cosmol. Astropart. Phys. 10 (2017) 046.

[65] D. G. Figueroa, S. Raatikainen, S. Rasanen, and E. Tomberg, Non-gaussian tail of the curvature perturbation in stochastic ultraslow-roll inflation: Implications for primordial black hole production, Phys. Rev. Lett. **127**, 101302 (2021).

[66] A. A. Starobinsky, Spectrum of adiabatic perturbations in the universe when there are singularities in the inflation potential, JETP Lett. **55**, 489 (1992).

[67] J. García-Bellido and E. Ruiz Morales, Primordial black holes from single field models of inflation, Phys. Dark Univ. **18**, 47 (2017).

[68] J. M. Ezquiaga, J. Garcia-Bellido, and E. Ruiz Morales, Primordial black hole production in critical Higgs inflation, Phys. Lett. B **776**, 345 (2018).

[69] H. Motohashi and W. Hu, Primordial black holes and slow-roll violation, Phys. Rev. D **96**, 063503 (2017).

[70] A. D. Linde, Hybrid inflation, Phys. Rev. D **49**, 748 (1994).

[71] P. Virtanen, R. Gommers, T. E. Oliphant, M. Haberland, T. Reddy, D. Cournapeau, E. Burovski, P. Peterson, W. Weckesser, J. Bright *et al.*, SciPy 1.0: Fundamental algorithms for scientific computing in Python, Nat. Methods **17**, 261 (2020).

[72] N. Yoshioka, T. Okubo, Y. Suzuki, Y. Koizumi, and W. Mizukami, Hunting for quantum-classical crossover in condensed matter problems, npj Quantum Inf. **10**, 45 (2024).